SANDIA REPORT
SAND2006-2845
Unlimited Release
Printed July 2006

Performance Characteristics of Cryofocusing GC/MS System at BWXT Pantex Plant

Jason R. Brown, Steven M. Thornberg, Judith F. Banet, Lorelei Woods and Jerry Ithaca

Prepared by
Sandia National Laboratories
Albuquerque, New Mexico 87185 and Livermore, California 94550

Sandia is a multiprogram laboratory operated by Sandia Corporation,
a Lockheed Martin Company, for the United States Department of Energy's
National Nuclear Security Administration under Contract DE-AC04-94AL85000.

Sandia National Laboratories

Issued by Sandia National Laboratories, operated for the United States Department of Energy by Sandia Corporation.

Printed in the United States of America. This report has been reproduced directly from the best available copy.

Available to DOE and DOE contractors from
U.S. Department of Energy
Office of Scientific and Technical Information
P.O. Box 62
Oak Ridge, TN 37831

Telephone: (865) 576-8401
Facsimile: (865) 576-5728
E-Mail: reports@adonis.osti.gov
Online ordering: http://www.osti.gov/bridge

Available to the public from
U.S. Department of Commerce
National Technical Information Service
5285 Port Royal Rd.
Springfield, VA 22161

Telephone: (800) 553-6847
Facsimile: (703) 605-6900
E-Mail: orders@ntis.fedworld.gov
Online order: http://www.ntis.gov/help/ordermethods.asp?loc=7-4-0#online

SAND 2006-2845
Unlimited Release
Printed July 2006

Performance Characteristics of Cryofocusing GC/MS System at BWXT Pantex Plant

Jason R. Brown, Steven M. Thornberg, and Judith F. Banet
Materials Aging and Reliability Department
Sandia National Laboratories
Albuquerque, NM 87185-0889

Lorelei Woods and Jerry Ithaca
Gas Analysis Laboratory
BWXT Pantex Plant
Amarillo, TX 79120-0020

Abstract

Ensuring the reliability of all components within a weapon system becomes increasingly important as the stockpile ages. One of the most noteworthy surveillance techniques designed to circumvent (or take place alongside) traditional D&I operations is to collect a sample of gas from within the internal atmosphere of a particular region in a weapon. While a wealth of information about the weapon may be encoded within the composition of its gas sample, our access to that information is only as good as the method used to analyze the sample. It has been shown that cryofocusing-GC/MS offers advantages in terms of sensitivity, ease of sample collection, and robustness of the equipment / hardware used.[1] Attention is therefore focused on qualifying a cryo-GC/MS system for routine stockpile surveillance operations at Pantex. A series of tests were performed on this instrument to characterize the linearity and repeatability of its response using two different standard gas mixes (ozone precursor and TO-14) at various concentrations. This paper outlines the methods used and the results of these tests in order to establish a baseline by which to compare future cryo-GC/MS analyses. A summary of the results is shown below.

Linearity Testing

Data set	Avg. Slope	Std. Deviation (%)	Avg. R^2 Value
OP: low concentration	753562	39%	0.9986
OP: high concentration	431227	34%	0.9141
OP: full range	679808	28%	0.8685
TO-14: low concentration	719545	47%	0.9931
TO-14: high concentration	413102	42%	0.9434
TO-14: full range	726094	48%	0.8449

Repeatability Testing

Data set	Std. Deviation (%)
OP: 0.5 cc	2.87%
OP: 10 cc	1.51%
TO-14: 0.5 cc	11.33%
TO-14: 10 cc	1.91%

Table of Contents

Table of Figures

Introduction

Ensuring the reliability of all components within a weapon system becomes increasingly important as the stockpile ages. Often, the accepted way to assess the condition of a particular weapon component is to employ disassembly and inspection (D&I) techniques, which are costly, time-consuming, and often destructive to the component being inspected. Alternatives to D&I operations are therefore highly desirable, especially those that could be employed in the field. One of the most noteworthy weapon surveillance techniques designed to circumvent (or take place alongside) traditional D&I operations is to collect a sample of gas from within the internal atmosphere of a particular region in a weapon. This gas subsequently undergoes chemical analysis, which can reveal a great deal of information about the state of the original weapon including the conditions under which it has been stored, the extent of hermeticity of the seals, and potentially how the weapon has aged. Gas sampling the internal atmosphere of a weapon or weapon component has many advantages in that it is fast, cost-effective, non-invasive, and can readily be employed in the field.

While a wealth of information about the weapon may be encoded within the composition of its gas sample, our access to that information is only as good as the method used to analyze the sample. In the past, a number of analytical techniques have been investigated for use to characterize the gas samples collected from weapons, including magnetic sector mass spectroscopy, solid phase microextraction (SPME), gas chromatography with a flame ionization detector (GC/FID), and cryofocusing gas chromatography / mass spectrometry (cryo-GC/MS).[1] Previous studies have been conducted to ascertain which of these methods reveals the most amount of information for trace organics from a weapon gas sample. GC/FID provides information about some small hydrocarbons (selected hydrocarbons containing less than 5 carbons) but is not configured to provide more. It has been shown that the method most suitable for sampling and analyzing a weapon atmosphere is cryo-GC/MS, as it offers advantages in terms of sensitivity, ease of sample collection, and robustness of the equipment / hardware used.[2] Attention is therefore focused on incorporating this analytical method into routine stockpile surveillance operations.

Currently, a cryo-GC/MS system at the BWXT Pantex Plant (a commercial HP5973 CG/MS with an Entech 7100 pre-concentrator and autosampler) is slated to become an integral part of the gas analysis activities that take place there. This system, developed under the Enhanced Surveillance Campaign (ESC) program,[3] will eventually perform organics analysis of samples captured in a gas sample bottles in the Enhanced Surveillance Campaign, the Core Surveillance program, weapon system samples, or any other component sample (component accelerated aging unit, etc.). However, before any analytical system can be incorporated into routine operations at Pantex, it must first undergo an Equipment Qualification (EQ) plan to demonstrate that it is operational within the required guidelines of sensitivity, repeatability, etc. In the case of the Pantex cryo-GC/MS system, an EQ plan was written to include studies which characterize the linearity, repeatability, and detection limits of the instrumentation.[3] A linearity study was additionally performed on a similar cryo-GC/MS system (Model 5973) at Sandia

National Laboratories, Org. 1822, to provide further information about the cryo-CG method. This report seeks to summarize the methods and results obtained in this series of tests, thus establishing a "baseline" of instrument performance.

Experimental

Instrumentation

The cryofocusing GC/MS at Pantex is comprised of three separate units: the cryofocusing unit (Entech model 7100 pre-concentrator and auto-sampler), the gas chromatograph (HP 6890 gas chromatograph), and the mass spectrometer with mass selective detector (HP5973). The GC column is a J&W scientific (Folsom, CA) DB-1 column, 0.25 mm x 50 m x .25 μm (film) with a split injection (5.0:1 ratio with a split flow of 7.5 ml/minute). Helium (6.0 grade) was used as the carrier gas for the GC at a flow rate of 1.5 ml/minute. The oven program is -10^{o}C for 5.5 minutes, 5 ^{o}C/min to 130 ^{o}C and hold for 5 minutes, followed by a second temperature ramp at 20 ^{o}C/ min to 220 ^{o}C, hold for 5 minutes. This GC/MS is capable of analyzing many of the semi-volatile organics. In cryofocusing GC/MS, a trap is cooled to -150 ^{o}C, an aliquot of the gas sample in drawn through the trap where volatile species are concentrated, and the trap is then rapidly heated to liberate the condensed organics into the GC. With this technique, excellent detection limits can be realized since the volume of gas drawn through the trap can be varied to adjust the mass of organics condensed.

Though the primary focus of the testing described herein pertains to the characterization (and qualification) of the cryofocusing GC/MS system at Pantex, an analogous system at Sandia National Labs underwent qualitative testing for linearity. This was done to show that the trends observed in the data from the system at Pantex are applicable to other similar systems, useful for demonstrating that the data trends are method, and not system dependent. The cryofocusing GC/MS system tested at Sandia (Org. 1825, Bldg. 701) is an Entech model 7100.

Test Matrix

To understand the behavior and response of any analytical instrument, it is useful to submit it to a series of tests in which the parameter or parameters of interest are varied. The focus of the Pantex cryo-GC/MS testing described herein was to determine how the instrument would respond to variations in the amount of sample condensed in the cryofocusing trap (i.e., the concentration of the sample). Also of interest was to verify that the instrument is capable of detecting a wide range of organic compounds. A test matrix was therefore designed in which the concentration of the analyte was varied over several orders of magnitude, enabling a determination to be made about the linearity of the instrument's response over that concentration range. Also, two specific analyte concentrations- one in the "high concentration" range and one in the "low concentration" range- were chosen and several repeated runs were performed at those settings, providing information about the repeatability of the instrument's response at set parameters. In the "low concentration" regime, the analyte gas was diluted by a factor of 100 with dry nitrogen, where as the gas in the "high concentration" regime did not undergo dilution.

Two different standard gas mixtures were used to conduct Pantex cryofocusing GC/MS tests: "ozone precursor (OP)" and "TO-14," both common organic gas standard mixes. Each of these gas standards consists of a suite of many organic compounds (mostly low molecular weight, common industrial organics) at low concentrations with a balance of nitrogen. In these studies, each of the organics contained in the OP and TO-14 existed at nominal concentrations of 1 part per million (ppm) in the original gas mixture. These gasses were procured through Matheson Tri-Gas, and the compositions were certified by the vendor (see **Appendix A**). For the qualification testing of the Pantex GC/MS, the test matrix described above was performed independently using both ozone precursor and TO-14. **Table 1** shows the original test matrix used.

(Note: In addition to the testing done on the Pantex instrument, tests were done on a similar instrument at Sandia National Laboratories to qualitatively characterize the linearity of the response with respect to concentration of the sample. These tests were performed using TO-14).

Table 1. Original Test Matrix for Cryo-GC/MS Qualification Study. Note: The test matrix was performed using Ozone Precursor and TO-14 gas standards.

Dilution factor	cc sampled	cc of original	Assumed MW	Mass captured (pg)
		Linearity Study		
1	20	20	200	4.464
1	10	10	200	2.232
1	5	5	200	1.116
1	2.5	2.5	200	0.558
100	100	1	200	0.223
100	50	0.5	200	0.112
100	25	0.25	200	0.056
100	10	0.1	200	0.022
		Repeatability Study		
1	10	10	200	2.232
1	10	10	200	2.232
1	10	10	200	2.232
1	10	10	200	2.232
100	50	0.5	200	0.112
100	50	0.5	200	0.112
100	50	0.5	200	0.112
100	50	0.5	200	0.112

The original test matrix is divided into two different concentration regimes: "high" and "low" concentration. In the low concentration regime, only very small amounts of the original sample gas were needed (1, .25, .5, and .1 cc of gas). However, the cryofocusing system is not capable of tightly controlling such small amounts of flow, and any error in the amount of gas captured in the cryo trap would be greatly magnified in the final results. Therefore, as a measure of maintaining the accuracy of the desired concentrations, the original standard gas was diluted by a factor of 100 with dry nitrogen prior to analysis. This allowed for a large amount of the diluted sample gas to be condensed by the cryofocusing unit (10, 25, 50, and 100 cc), resulting in a much tighter control of the "low concentration" regime in the test matrix.

Adherence to Qualification Documents

Section 4.6 of SS306587AJ "Process Requirements for Sampling and Analysis of Gas Samples from Internal Weapon Atmospheres" states that new gas analysis techniques applied to stockpile surveillance (including cryofocusing GC/MS) must undergo two studies before they can be added to the list of accepted methods.[4] These two requirements are:

1. "*Before these techniques can be added to this requirement, a study of their impact, if any, on water vapor measurement must be conducted and added to this SS*."
2. "*…a study of the technique's impact on the Sequence of Operations in Section 4.2.4 must also be conducted and is subject to a requalification requirement if necessary*."

In the case of cryofocusing CG/MS, these two points are easily addressed. First, the water vapor measurement will not be affected, as the gas sampling takes place after the frost point measurement in the sampling procedure (as outlined in **Figure 1** of SS306587AJ). Second, the gas sample needed for cryo-GC/MS is extracted during the accepted procedure outlined in **Figure 1** of SS306587AJ; that is, collecting a gas sample for cryo GC/MS entails simply opening an evacuated gas sample bottle, which has no impact on the existing procedure whatsoever. (This is in contrast to a method such as SPME, which requires that the collection fiber remain exposed to the internal atmosphere of the component for a more prolonged period.[5])

Results

Each of the two gas standards (ozone precursor and TO-14) was used to perform the test matrix (shown in Table I) on the Pantex cryofocusing GC/MS system. In each of the runs, total ion concentration (TIC) values were generated by the mass spectrometer for each individual organic compound retained in the cryofocusing trap (and later separated in the GC column). These TIC peaks are a direct measure of the total signal intensity generated by a particular organic compound in the sample. A typical GC/MS chromatogram with TIC peaks is shown in **Figure 1**. Since each organic compound in the analyte gas generates a unique TIC peak at a certain retention time in the chromatogram, trends in individual TIC peak intensities can be tracked over the various tests performed in the test matrix. This is what ultimately provides information about the linearity and repeatability exhibited by the instrument. Tables with the peak identification information for each of the gas standards can be found in **Appendix B**.

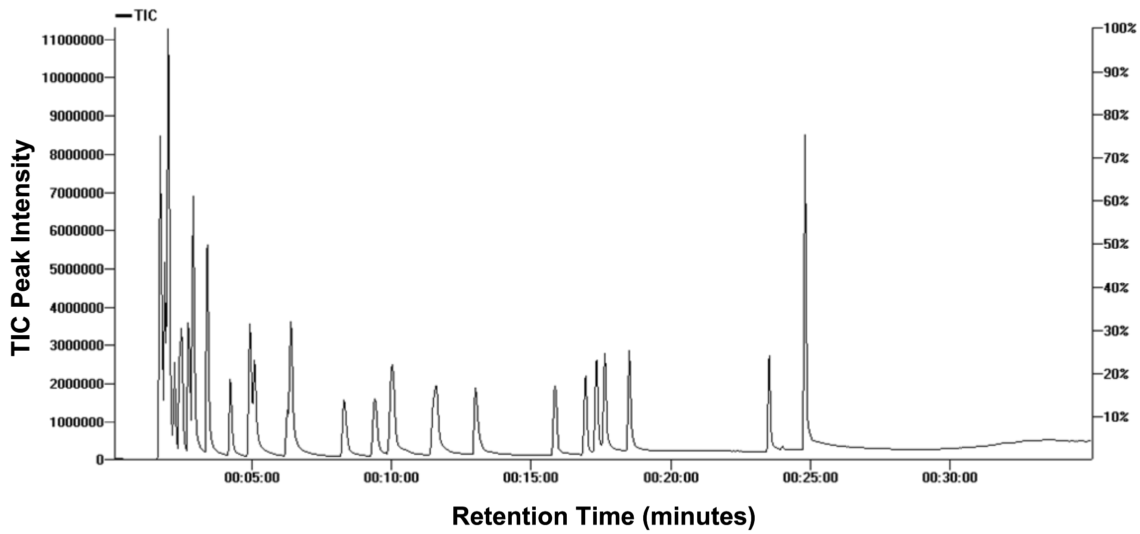

Figure 1. Gas chromatogram showing TIC peaks.
Each peak in the plot above represents a unique component separated out in the GC column.

Linearity Testing

The ability of the cryo-GC/MS instrument to produce linear results is investigated by plotting the TIC intensities of the individual peaks over the range of sample concentrations used in the test matrix. These plots are summarized on the following pages (**Figure 2**: Ozone Precursor, low concentration range. **Figure 3**: Ozone Precursor, high concentration range. **Figure 4**: TO-14, low concentration range. **Figure 5**: TO-14, high concentration range. **Table 2**: Statistical Summary of Linearity Testing.) Note: Tabulated data and plots for low, high, and full concentration ranges are given in **Appendix C**. In **Figures 2 -5**, each curve represents a peak at a specific retention time in the chromatogram. Legends and obvious outlying points were omitted in these plots.):

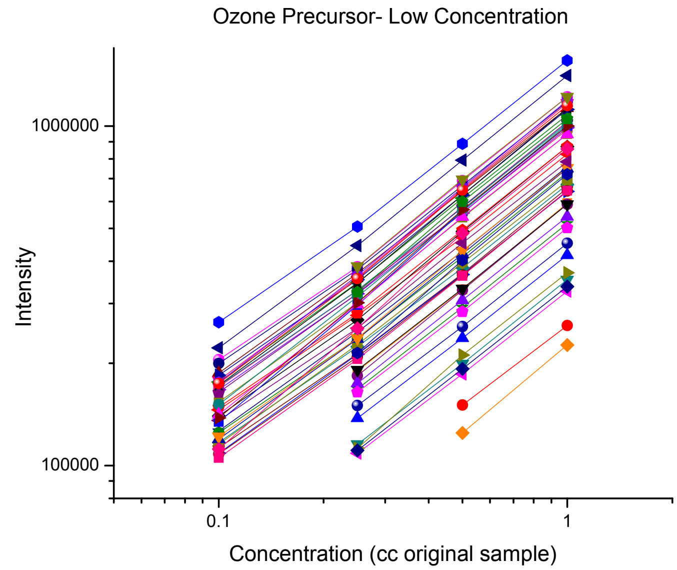

Figure 2. Cryo-GC/MS response over low concentration range of Ozone Precursor. Each curve represents a unique compound separated out in the gc column.

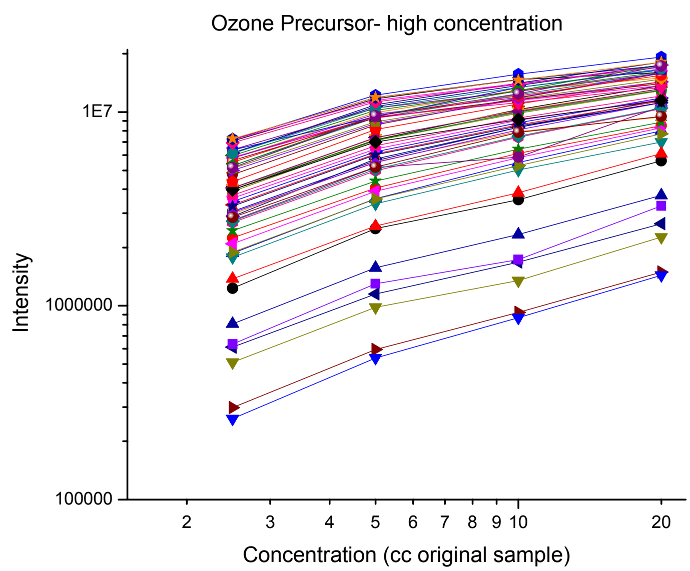

Figure 3. Cryo-GC/MS response over high concentration range of Ozone Precursor. Each curve represents a unique compound separated out in the gc column.

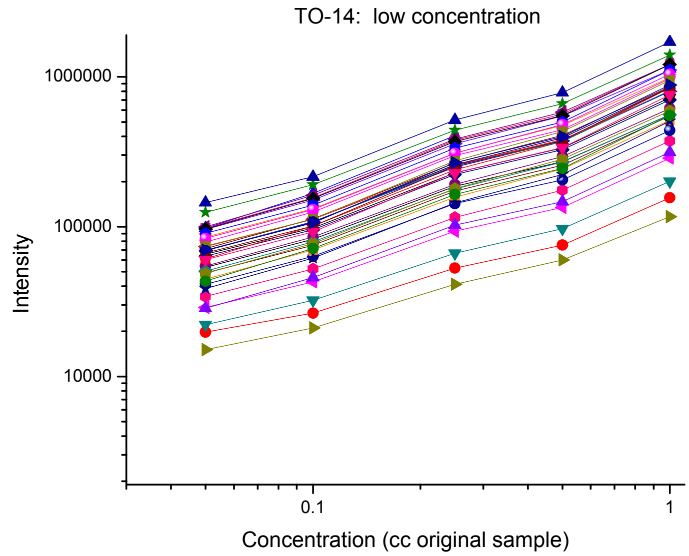

Figure 4. Cryo-GC/MS response over low concentration range of TO-14. Each curve represents a unique compound separated out in the gc column.

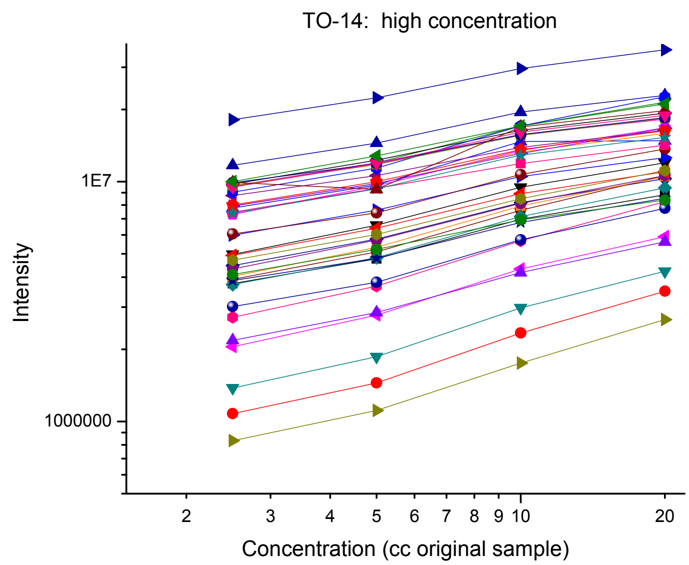

Figure 5. Cryo-GC/MS response over high concentration range of TO-14. Each curve represents a unique compound separated out in the gc column.

Table 2. Statistical Summary of Linearity Testing. The Average R2 values are calculated for the low, high, and full concentration ranges by averaging the R2 value for each of the individual peaks in the data set.

Linearity Testing

Data set	Avg. Slope	Std. Deviation (%)	Avg. R^2 Value
OP: low concentration	753562	39%	0.9986
OP: high concentration	431227	34%	0.9141
OP: full range	679808	28%	0.8685
TO-14: low concentration	719545	47%	0.9931
TO-14: high concentration	413102	42%	0.9434
TO-14: full range	726094	48%	0.8449

Linearity Testing- Discussion

As expected, the data from both the ozone precursor and TO-14 outline a direct proportionality between sample concentration and signal intensity. However, the difference in the shape of the curves (i.e slope) between high and low concentration is quite pronounced. This is true for both ozone precursor and TO-14. The difference becomes even more apparent when a least-squares linear fit is applied across the entire concentration range, in which case the R^2 value for the linear fit drops to ~ .87 and ~.84 for ozone precursor and TO-14, respectively (see **Table 2**). The reassuring thing to note is that the slopes for all of the peaks are relatively constant within the two concentration ranges, and the minor deviations from linearity are consistent for all the peaks in the chromatogram. These deviations and the differences in slope values between concentration ranges can most likely be attributed to discrepancies in the dilution factor and / or the measured volume of the analyte, rather than some inherent effect exhibited by the instrument.

Repeatability Testing

The ability of the cryo-GC/MS instrument to produce repeatable results is investigated by plotting the TIC intensities of the individual peaks at a set sample concentration. These plots are shown on the following pages (**Figure 6**: Ozone Precursor, low concentration. **Figure 7**: Ozone Precursor, high concentration. **Figure 8**: TO-14, low concentration. **Figure 9**: TO-14, high concentration.) Note: Tabulated data and plots for repeatability tests are given in **Appendix D**. In **Figures 6-9**, each curve represents a peak at a specific retention time in the chromatogram. Legends and obvious outlying were omitted in these plots. A summary of the results is given in **Table 3**.

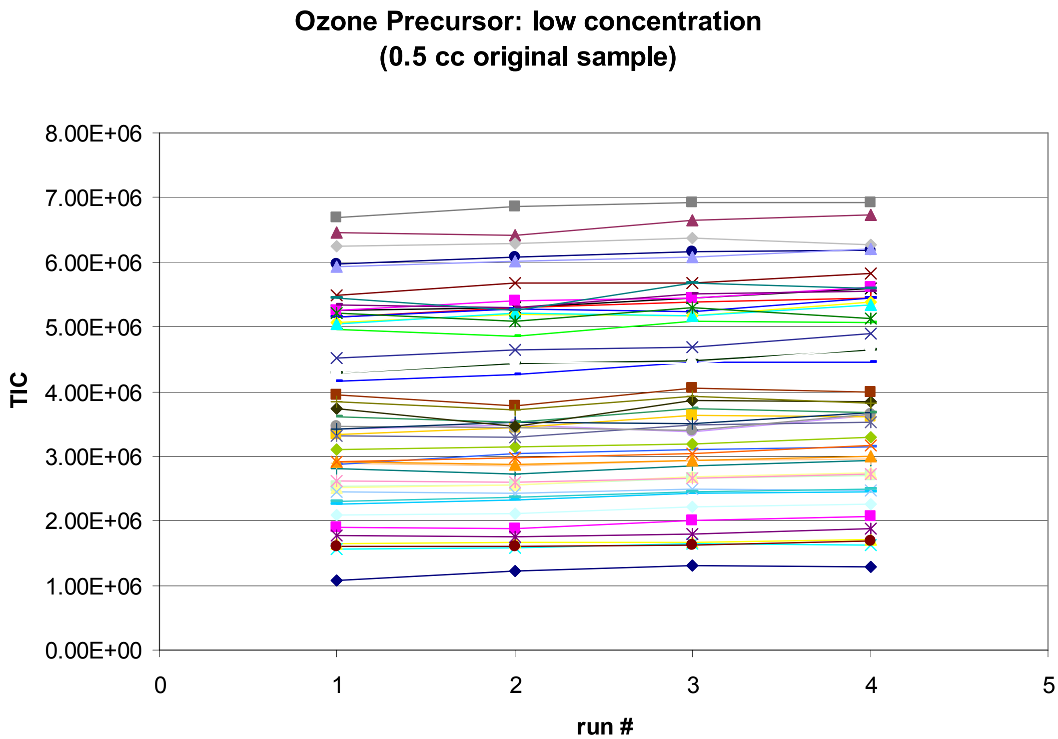

Figure 6. Cryo-GC/MS response at low concentration (0.5 cc original sample) Ozone Precursor.

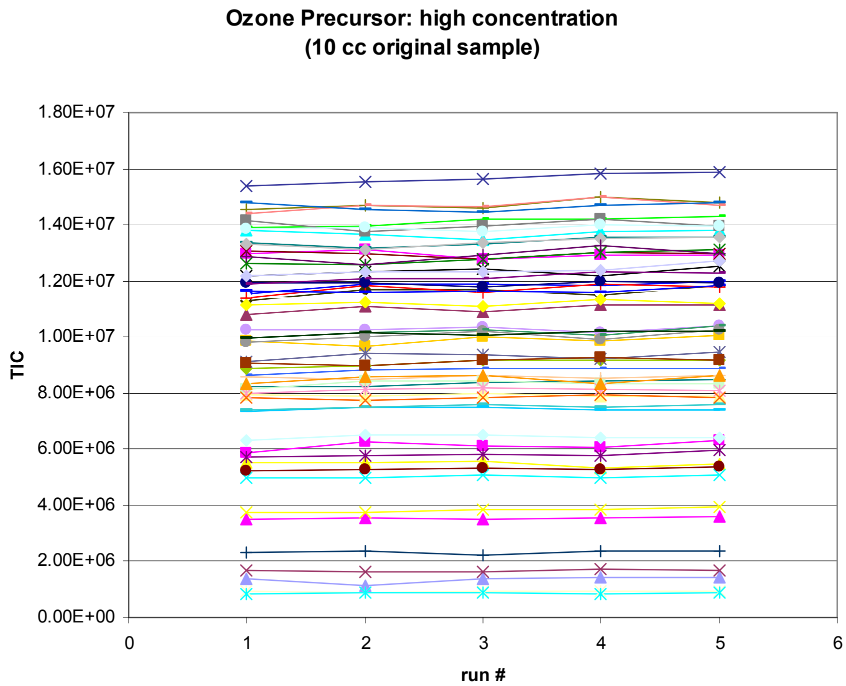

Figure 7. Cryo-GC/MS response at high concentration (10 cc original sample) Ozone Precursor.

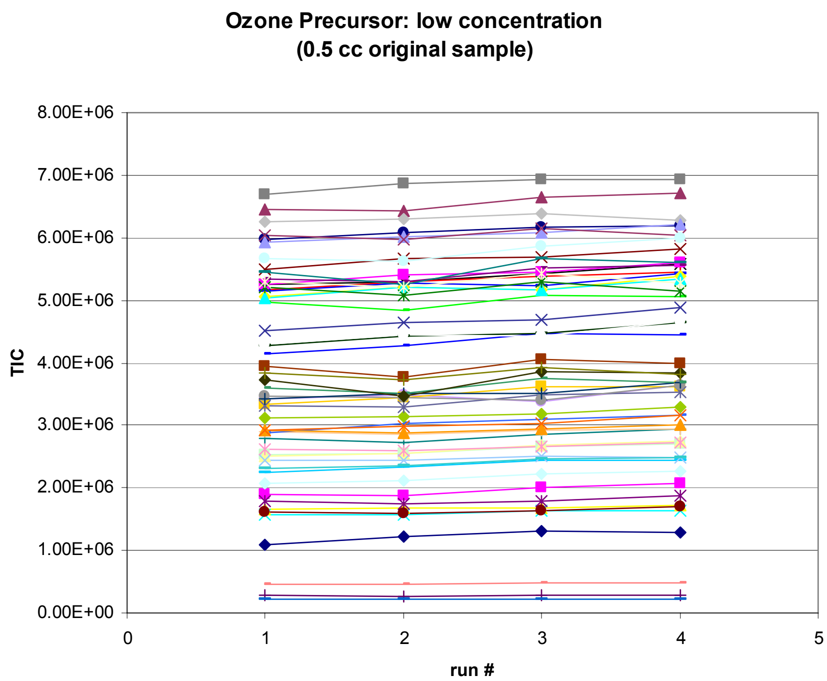

Figure 8. Cryo-GC/MS response at low concentration (0.5 cc original sample) TO-14.

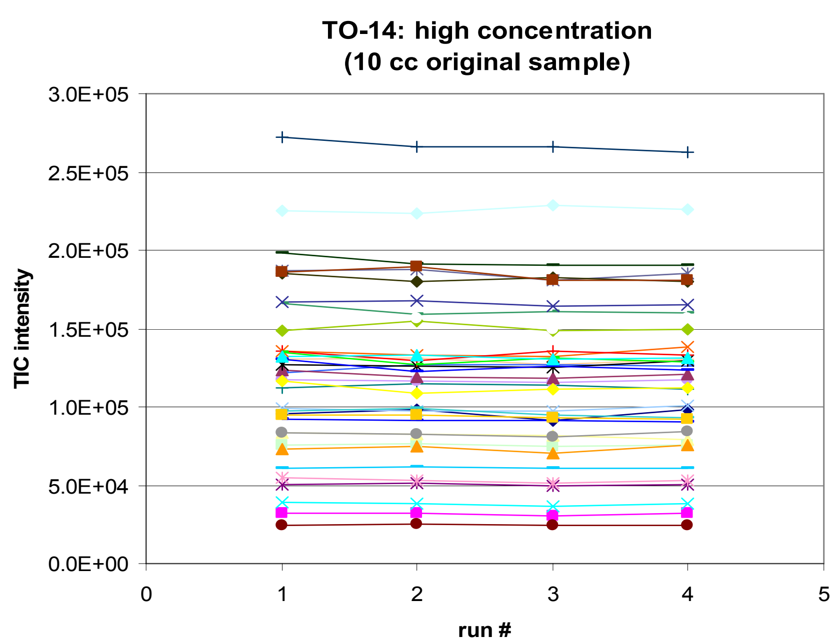

Figure 9. Cryo-GC/MS response at high concentration (10 cc original sample) TO-14.

Table 3. Cryo-GC/MS Repeatability and Linearity Testing: Summary of results. Note: "Avg. % Deviation" is defined as the Standard Deviation / Mean of the peak heights multiplied by 100%.

Repeatability Testing

Data set	Std. Deviation (%)
OP: 0.5 cc	2.87%
OP: 10 cc	1.51%
TO-14: 0.5 cc	11.33%
TO-14: 10 cc	1.91%

Cryo-GC/MS system at Sandia National Laboratories

In addition to the testing done on the Pantex instrument, tests were done on a similar instrument at Sandia National Laboratories to qualitatively characterize the linearity of the response with respect to concentration of the sample. These tests were performed using TO-14. The results of this test, useful from a qualitative standpoint to demonstrate the overall response of an instrument similar to the cryo-GC/MS at Pantex, are shown below in **Figure 10**. It can be seen that the response is highly linear for all the peaks observed.

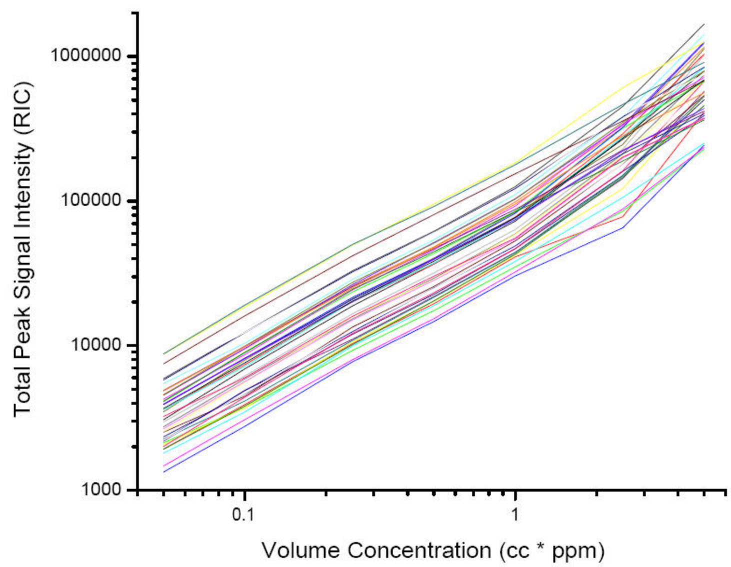

Figure 10. Linearity testing performed on cryo-GC/MS system at Sandia.

Conclusions

Cryo-GC/MS has been shown to have many advantages over alternative methods for trace organics analysis of gas samples taken from the internal atmospheres of weapon components. Some notable advantages are:

- The technology associated with cryo-GC/MS is mature and accepted.
- The sampling procedure is fast, simple, and employs robust hardware.
- Once a sample is taken, it remains viable for months.
- Cryo-GC/MS exhibits excellent sensitivity with minimal background interferences.

The data presented in this paper summarizes the testing done on a cryo-GC/MS system at Pantex in order to characterize its performance and qualify it for routine use in stockpile surveillance. This data set is meant to serve as a baseline by which to compare future data collected using this technique.

References

1. Thornberg, S. M. and Jarek, R. L., “Comparison of Weapon Organic Gas Sampling and Analysis Methods”, SAND99-2738, October, 1999.

2. Thornberg, S. M. and Jarek, R.L., “Comparison of Gas Sampling and Analysis Methods”, Power Point Presentation given at the US-UK Focused Exchange on “Capsule Atmosphere Sampling and Analysis”, November 16, 1999.

3. Dahms, G. E. and Jennings-Williams, “Qualification Plan: Pantex Cryo-Focusing Gas Chromatograph / Mass Spectrometer”, Qualification Plan Document PQ1A3417, September, 2004.

4. Chavez, S., “Process Requirements for Sampling and Analysis of Gas Samples from Internal Weapon Atmospheres”, SS306857AJ, October, 2003.

5. Chambers, D. M., “Solid Phase Microextraction for the Analysis of Nuclear Weapons”, LLNL document #UCRL-IC-132600, Aug. 16, 1998.

Appendix A. Vendor Certification of Gas Standard Composition.

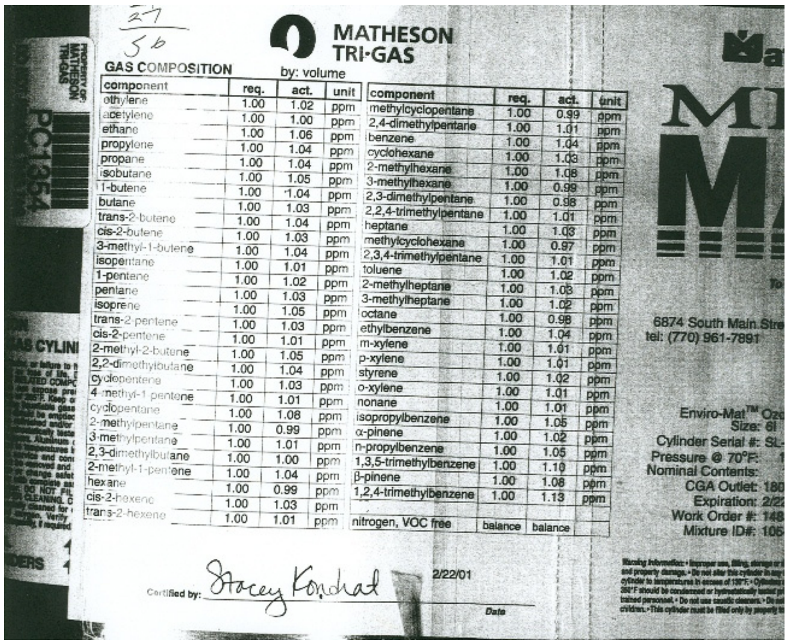

MATHESON TRI-GAS

GAS COMPOSITION by: volume

component	req.	act.	unit
ethylene	1.00	1.02	ppm
acetylene	1.00	1.00	ppm
ethane	1.00	1.06	ppm
propylene	1.00	1.04	ppm
propane	1.00	1.04	ppm
isobutane	1.00	1.05	ppm
1-butene	1.00	1.04	ppm
butane	1.00	1.03	ppm
trans-2-butene	1.00	1.04	ppm
cis-2-butene	1.00	1.03	ppm
3-methyl-1-butene	1.00	1.04	ppm
isopentane	1.00	1.01	ppm
1-pentene	1.00	1.02	ppm
pentane	1.00	1.03	ppm
isoprene	1.00	1.05	ppm
trans-2-pentene	1.00	1.03	ppm
cis-2-pentene	1.00	1.01	ppm
2-methyl-2-butene	1.00	1.05	ppm
2,2-dimethylbutane	1.00	1.04	ppm
cyclopentene	1.00	1.03	ppm
4-methyl-1-pentene	1.00	1.01	ppm
cyclopentane	1.00	1.08	ppm
2-methylpentane	1.00	0.99	ppm
3-methylpentane	1.00	1.01	ppm
2,3-dimethylbutane	1.00	1.00	ppm
2-methyl-1-pentene	1.00	1.04	ppm
hexane	1.00	0.99	ppm
cis-2-hexene	1.00	1.03	ppm
trans-2-hexene	1.00	1.01	ppm
methylcyclopentane	1.00	0.99	ppm
2,4-dimethylpentane	1.00	1.01	ppm
benzene	1.00	1.04	ppm
cyclohexane	1.00	1.03	ppm
2-methylhexane	1.00	1.08	ppm
3-methylhexane	1.00	0.99	ppm
2,3-dimethylpentane	1.00	0.98	ppm
2,2,4-trimethylpentane	1.00	1.01	ppm
heptane	1.00	1.03	ppm
methylcyclohexane	1.00	0.97	ppm
2,3,4-trimethylpentane	1.00	1.01	ppm
toluene	1.00	1.02	ppm
2-methylheptane	1.00	1.03	ppm
3-methylheptane	1.00	1.02	ppm
octane	1.00	0.98	ppm
ethylbenzene	1.00	1.04	ppm
m-xylene	1.00	1.01	ppm
p-xylene	1.00	1.01	ppm
styrene	1.00	1.02	ppm
o-xylene	1.00	1.01	ppm
nonane	1.00	1.01	ppm
isopropylbenzene	1.00	1.05	ppm
α-pinene	1.00	1.02	ppm
n-propylbenzene	1.00	1.05	ppm
1,3,5-trimethylbenzene	1.00	1.10	ppm
β-pinene	1.00	1.08	ppm
1,2,4-trimethylbenzene	1.00	1.13	ppm
nitrogen, VOC free	balance	balance	

Certified by: Stacey Kondhat 2/22/01 Date

Ozone Precursor

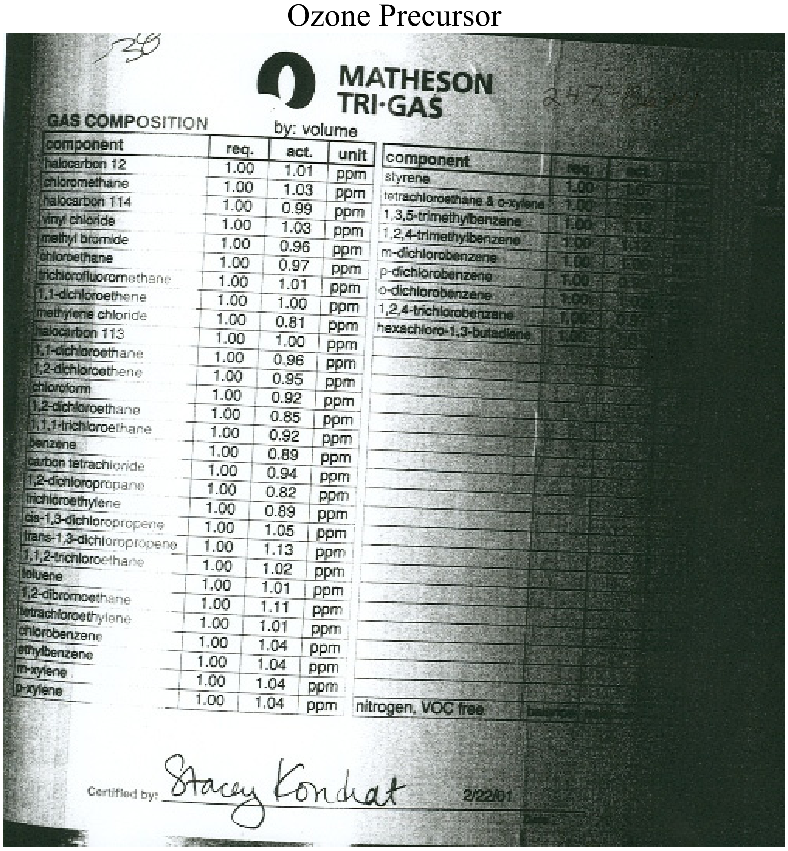

MATHESON TRI-GAS

GAS COMPOSITION by: volume

component	req.	act.	unit
halocarbon 12	1.00	1.01	ppm
chloromethane	1.00	1.03	ppm
halocarbon 114	1.00	0.99	ppm
vinyl chloride	1.00	1.03	ppm
methyl bromide	1.00	0.96	ppm
chloroethane	1.00	0.97	ppm
trichlorofluoromethane	1.00	1.01	ppm
1,1-dichloroethene	1.00	1.00	ppm
methylene chloride	1.00	0.81	ppm
halocarbon 113	1.00	1.00	ppm
1,1-dichloroethane	1.00	0.96	ppm
1,2-dichloroethene	1.00	0.95	ppm
chloroform	1.00	0.92	ppm
1,2-dichloroethane	1.00	0.85	ppm
1,1,1-trichloroethane	1.00	0.92	ppm
benzene	1.00	0.89	ppm
carbon tetrachloride	1.00	0.94	ppm
1,2-dichloropropane	1.00	0.82	ppm
trichloroethylene	1.00	0.89	ppm
cis-1,3-dichloropropene	1.00	1.05	ppm
trans-1,3-dichloropropene	1.00	1.13	ppm
1,1,2-trichloroethane	1.00	1.02	ppm
toluene	1.00	1.01	ppm
1,2-dibromoethane	1.00	1.11	ppm
tetrachloroethylene	1.00	1.01	ppm
chlorobenzene	1.00	1.04	ppm
ethylbenzene	1.00	1.04	ppm
m-xylene	1.00	1.04	ppm
p-xylene	1.00	1.04	ppm
styrene	1.00	[illegible]	[illegible]
tetrachloroethane & o-xylene	1.00	[illegible]	[illegible]
1,3,5-trimethylbenzene	1.00	[illegible]	[illegible]
1,2,4-trimethylbenzene	1.00	[illegible]	[illegible]
m-dichlorobenzene	1.00	[illegible]	[illegible]
p-dichlorobenzene	1.00	[illegible]	[illegible]
o-dichlorobenzene	1.00	[illegible]	[illegible]
1,2,4-trichlorobenzene	1.00	[illegible]	[illegible]
hexachloro-1,3-butadiene	1.00	[illegible]	[illegible]
nitrogen, VOC free	[illegible]	[illegible]	

Certified by: Stacey Kondhat 2/22/01 Date

TO-14

Appendix B. Gas Standard Compositions and Peak Identification Table.

Ozone Precursor Gas Standard

Peak #	Component
Not seen	ethylene
Not seen	acetylene
Not seen	ethane
1	propylene
Not seen	propane
2	isobutane
3	1-butene
4	n-butane
5	trans-2-butene
6	cis-2-butene
7	3-methyl-1-butene
8	isopentane
9	1-pentene
10	n-pentane
11	isoprene
12	trans-2-pentene
13	cis-2-pentene
14	2-methyl-2-butene
15	2,2-dimethylbutane
16	cyclopentene
17	4-methyl-1-pentene
18	cyclopentane
19	2-methylpentane
20	3-methylpentane
21	2,3-dimethylbutane
22	2-methyl-1-pentene
23	n-hexane
24	cis-2-hexene
25	trans-2-hexene
26	methylcyclopentane
27	2,4-dimethylpentane
28	benzene
29	cyclohexane
30	2-methylhexane
31	3-methylhexane
Not seen	2,3-dimethylpentane
32	2,2,4-trimethylpentane
33	n-heptane
34	methylcyclohexane
35	2,3,4-trimethylpentane
36	toluene
37	2-methylheptane
38	3-methylheptane
39	n-octane
40	ethylbenzene
41	p-xylene
42	m-xylene
43	styrene
44	o-xylene
45	n-nonane
46	isopropylbenzene
47	alpha-pinene
48	n-propylbenzene
49	1,3,5-trimethylbenzene
50	beta-pinene
51	1,2,4-trimethylbenzene

TO-14 Gas Standard

Peak #	Component
1	dichlorodifluoromethane (Freon 12)
2	methyl chloride
3	1,1-dichloro-1,2,2,2-tetrafluoroethane (Freon 114)
4	vinyl chloride
5	methyl bromide
6	Chloroethane
7	trichlorofluoromethane
8	1,1-dichloroethene
9	Methylene Chloride
10	1,1,2 - trifluoro-1,2,2-trichloroethane (Freon 113)
11	1,1-dichloroethane
12	cis-1,2-dichloroethene
13	cloroform
14	1,2-dichloroethane
15	1,1,1-trichloroethane
16	benzene
17	carbon tetrachloride
18	1,2-dichloropropane
19	trichloroethylene
20	cis-1,3-dichloropropylene
21	trans-1,3-dichloropropylene
22	1,1,2-trichloroethane
23	toluene
24	1,2-dibromoethane
25	tetrachloroethylene
26	chlorobenzene
27	ethylbenzene
28	m-xylene
29	p-xylene
30	styrene
31	o-xylene & Tetrachloroethane
32	1,3,5-trimethylbenzene
33	1,2,4-trimethylbenzene
34	m-dichlorobenzene
35	p-dichlorobenzene
36	o-dichlorobenzene
37	1,2,4-trichlorobenzene
38	hexachloro-1,3-butadiene

Appendix C. Plots and Data of Linearity Testing

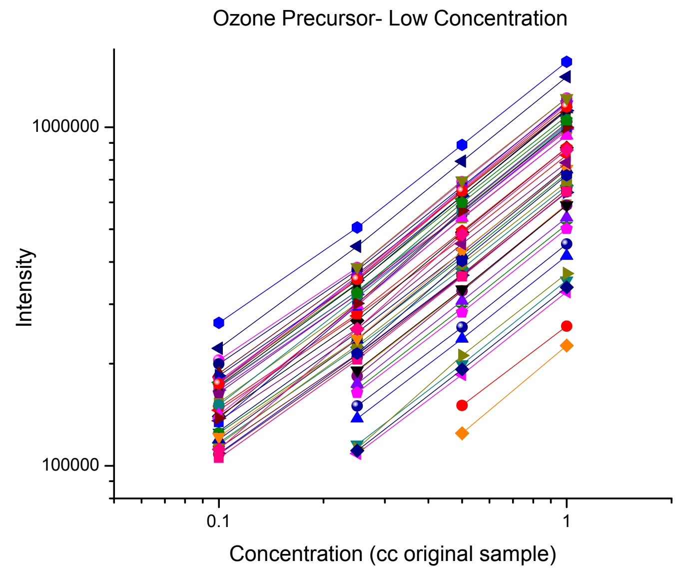

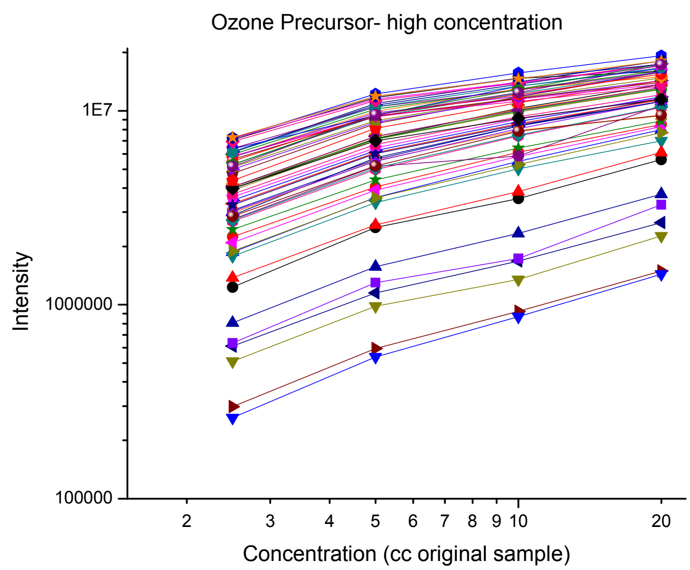

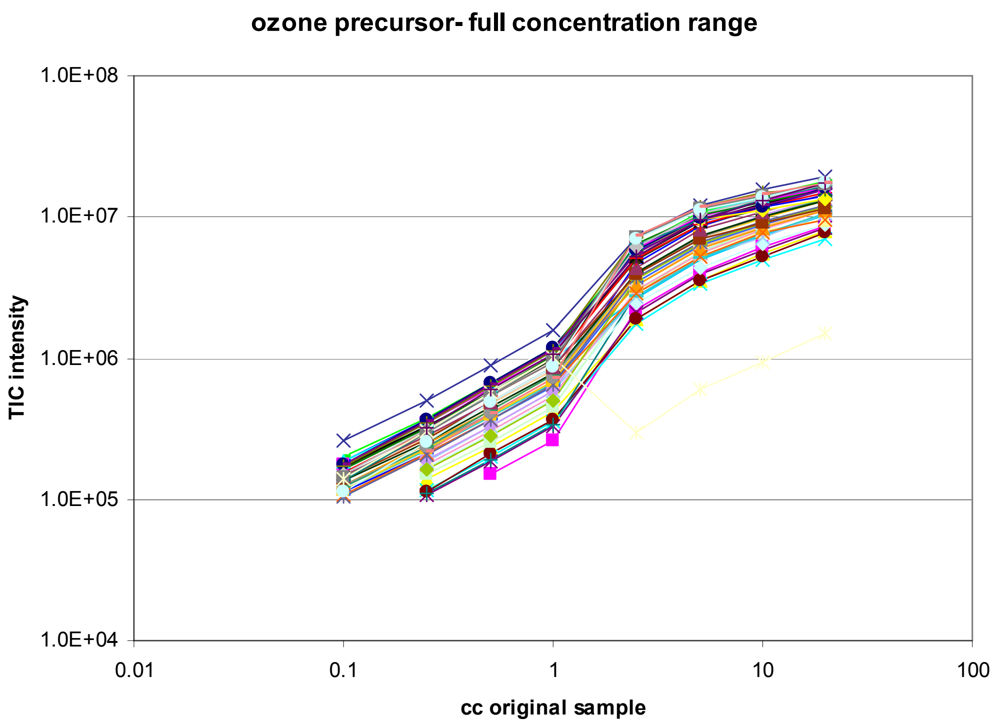
ozone precursor- full concentration range
1.0E+08
1.0E+07
1.0E+06
1.0E+05
1.0E+04
TIC intensity
0.01
0.1
1
10
100
cc original sample

Ozone Precursor: Low Concentration

Concentration:	0.1	0.25	0.5	1	SLOPE	INTERCEPT	R2
peak 1							
peak 2	-	--	150661	258410	215498	42912	1.0000
peak 3	--	137819	237390	416674	369915	48177	0.9993
peak 4	--	115499	199347	352550	314688	38898	0.9995
peak 5	--	108585	185938	326148	288703	38480	0.9994
peak 6	--	112324	211663	369903	339587	33204	0.9965
peak 7	--	110777	192434	336449	299058	38769	0.9990
peak 8	112700	213353	367522	656650	600889	59645	0.9992
peak 9	170403	327832	555953	978011	889090	96846	0.9984
peak 10	--	168081	292523	515964	461421	56360	0.9993
peak 11	--	150079	256547	451842	400671	52431	0.9995
peak 12	--	189759	330327	592047	534535	58899	0.9997
peak 13	--	183759	328678	587986	536062	54105	0.9992
peak 14	--	174766	306938	541497	486138	57486	0.9991
peak 15	--	191121	331876	588681	527727	62718	0.9995
peak 16	145907	277156	470266	827723	751270	82801	0.9986
peak 17	108636	212677	364986	641332	586514	60645	0.9981
peak 18	116830	223658	381898	672944	612906	65364	0.9986
peak 19	--	164470	283809	500961	446605	55894	0.9994
peak 20	115490	227244	394723	689424	632317	64274	0.9977
peak 21	126480	247447	427612	760248	698768	67267	0.9987
peak 22	108060	209130	363828	643529	591012	57794	0.9986
peak 23	105343	205673	361829	645145	596394	53665	0.9988
peak 24	124890	236722	411643	730383	669219	66396	0.9989
peak 25	119543	235972	420109	750644	697717	58873	0.9988
peak 26	121707	237432	429687	753256	699149	62164	0.9978
peak 27	135636	253715	452101	785301	719616	73866	0.9979
peak 28	167222	320433	554743	990320	909001	87767	0.9991
peak 29	139857	268616	488907	869937	809951	67227	0.9987
peak 30	148402	280824	493468	870809	799131	78778	0.9987
peak 31	264153	505713	886273	1.56E+06	1430640	142091	0.9984
peak 32	171276	328229	575296	1.02E+06	939380	89509	0.9988
peak 33	205169	384887	690560	1.22E+06	1129736	103563	0.9988
peak 34	153538	302371	537625	947066	876675	79688	0.9981
peak 35	199707	378292	667778	1.18E+06	1085564	104516	0.9987
peak 36	187408	368657	643313	1.13E+06	1043170	100718	0.9982
peak 37	178108	358549	653090	1.17E+06	1103498	80772	0.9988
peak 38	176314	345283	613023	1.08E+06	999825	91511	0.9983
peak 39	184464	352565	626591	1.12E+06	1037196	91449	0.9991
peak 40			124559	226202	203286	22916	1.0000
peak 41	164005	321198	577753	1.03E+06	962239	78976	0.9988
peak 42	175718	362684	659609	1.19E+06	1123751	77761	0.9988
peak 43	172284	344002	626354	1.13E+06	1055701	78768	0.9988
peak 44	174304	355329	647728	1.15E+06	1078255	83002	0.9980
peak 45	134389	296952	562328	1.00E+06	962242	54533	0.9974
peak 46	151336	314503	561307	1.01E+06	950489	70396	0.9987
peak 47	141392	298612	540282	945819	886594	71476	0.9968
peak 48		386453	696243	1.22E+06	1105113	123580	0.9982
peak 49	222035	444391	793089	1.41E+06	1315452	109660	0.9985
peak 50	138235	301844	566786	1.00E+06	956605	60269	0.9970
peak 51	111734	253530	483609	856634	822913	45780	0.9965
peak 52		323796	598567	1.05E+06	964271	96209	0.9977
peak 53		214575	402541	720536	669097	55577	0.9982
peak 54							
			AVERAGE:		753562	AVERAGE:	0.9986
			std dev		292772.02		
			%		38.851732		

Ozone Precursor: High Concentration

Concentration:	2.5	5	10	20	SLOPE	INTERCEPT	R2
peak 1							
peak 2	2.24E+06	4.05E+06	6.13E+06	8.50E+06	339942	2041879	0.9495
peak 3	1.87E+06	3.57E+06	5.48E+06	8.00E+06	333355	1605512	0.9628
peak 4	1.78E+06	3.36E+06	5.02E+06	7.01E+06	282303	1643870	0.9466
peak 5	2.09E+06	3.90E+06	5.81E+06	8.30E+06	335917	1873651	0.9560
peak 6	1.89E+06	3.56E+06	5.29E+06	7.71E+06	315592	1655258	0.9616
peak 7	2.90E+06	5.73E+06	8.36E+06	1.12E+07	442182	2905435	0.9228
peak 8	4.75E+06	8.58E+06	1.18E+07	1.58E+07	582857	4767244	0.9253
peak 9	2.69E+06	4.98E+06	7.42E+06	1.04E+07	414901	2476343	0.9492
peak 10	2.44E+06	4.41E+06	6.42E+06	8.87E+06	345931	2294883	0.9459
peak 11	3.07E+06	5.61E+06	8.34E+06	1.16E+07	460064	2837355	0.9481
peak 12	2.98E+06	5.54E+06	7.92E+06	9.44E+06	337046	3311807	0.8506
peak 13	2.76E+06	5.18E+06	5.85E+06	1.07E+07	420748	2176469	0.9599
peak 14	3.03E+06	5.49E+06	8.10E+06	1.12E+07	441696	2817777	0.9470
peak 15	3.97E+06	7.19E+06	1.03E+07	1.37E+07	519721	3918543	0.9283
peak 16	3.32E+06	6.08E+06	8.57E+06	1.14E+07	431062	3309736	0.9259
peak 17	3.45E+06	6.23E+06	8.80E+06	1.18E+07	443773	3405884	0.9300
peak 18	2.73E+06	5.07E+06	7.51E+06	1.05E+07	418651	2527831	0.9482
peak 19	3.59E+06	6.45E+06	9.07E+06	1.16E+07	425313	3700044	0.9071
peak 20	3.89E+06	7.12E+06	9.88E+06	1.29E+07	477615	3981446	0.9142
peak 21	3.27E+06	6.02E+06	8.49E+06	1.12E+07	421110	3299374	0.9204
peak 22	2.86E+06	5.20E+06	7.85E+06	9.49E+06	352502	3043600	0.8719
peak 23	3.72E+06	6.71E+06	9.33E+06	1.21E+07	443073	3818426	0.9123
peak 24	4.05E+06	7.15E+06	1.00E+07	1.30E+07	475148	4109737	0.9151
peak 25	806663	1.57E+06	2.33E+06	3.72E+06	159074	614697	0.9810
peak 26	4.05E+06	7.36E+06	1.02E+07	1.32E+07	484164	4169050	0.9110
peak 27	4.06E+06	7.39E+06	1.01E+07	1.32E+07	481554	4181537	0.9125
peak 28	5.00E+06	8.74E+06	1.16E+07	1.43E+07	478945	5403782	0.8743
peak 29	3.98E+06	6.99E+06	9.14E+06	1.15E+07	386363	4267075	0.8846
peak 30	4.37E+06	8.13E+06	1.10E+07	1.43E+07	520866	4577037	0.9049
peak 31	7.19E+06	1.22E+07	1.57E+07	1.92E+07	619811	7750840	0.8741
peak 32	5.29E+06	9.36E+06	1.23E+07	1.58E+07	547179	5563453	0.8997
peak 33	5.85E+06	9.31E+06	1.15E+07	1.37E+07	402274	6334496	0.8554
peak 34	5.11E+06	8.91E+06	1.17E+07	1.48E+07	505679	5401300	0.8954
peak 35	6.10E+06	1.09E+07	1.41E+07	1.81E+07	618540	6493998	0.8933
peak 36	5.63E+06	9.36E+06	1.16E+07	1.40E+07	424377	6175322	0.8508
peak 37	5.79E+06	9.47E+06	1.12E+07	1.34E+07	380436	6401076	0.8350
peak 38	5.95E+06	1.02E+07	1.29E+07	1.61E+07	520534	6398558	0.8792
peak 39	6.16E+06	1.07E+07	1.37E+07	1.75E+07	588976	6498716	0.8978
peak 40	5.79E+06	9.93E+06	1.30E+07	1.50E+07	467160	6531837	0.8186
peak 41	6.39E+06	1.05E+07	1.28E+07	1.58E+07	481539	6859516	0.8750
peak 42	5.78E+06	9.75E+06	1.19E+07	1.60E+07	526212	5915664	0.9201
peak 43	7.09E+06	1.17E+07	1.47E+07	1.60E+07	440010	8238182	0.7424
peak 44	5.51E+06	9.58E+06	1.21E+07	1.55E+07	514794	5855201	0.8936
peak 45	6.36E+06	9.47E+06	1.34E+07	1.65E+07	548450	6289595	0.9139
peak 46	6.11E+06	1.05E+07	1.34E+07	1.67E+07	546895	6554303	0.8832
peak 47	7.20E+06	1.15E+07	1.40E+07	1.70E+07	499094	7735002	0.8672
peak 48	510905	982282	1.35E+06	2.26E+06	94669	388461	0.9826
peak 49	610635	1.15E+06	1.68E+06	2.65E+06	111153	480873	0.9799
peak 50	297926	595140	9.25E+05	1.49E+06	65575	212794	0.9830
peak 51	6.94E+06	1.13E+07	1.39E+07	1.75E+07	545102	7309357	0.8942
peak 52	5.29E+06	9.54E+06	1.29E+07	1.75E+07	645950	5262070	0.9315
peak 53	7.27E+06	1.19E+07	1.47E+07	1.74E+07	512217	8017260	0.8400
peak 54	7.29E+06	1.19E+07	1.46E+07	1.81E+07	554890	7775090	0.8802
peak 55	5.17E+06	9.54E+06	1.24E+07	1.73E+07	637284	5126299	0.9360
peak 56	634341	1.30E+06	1.73E+06	3.28E+06	143905	387724	0.9839
peak 57	1.23E+06	2.50E+06	3.53E+06	5.60E+06	235098	1011418	0.9732
peak 58	1.38E+06	2.58E+06	3.83E+06	6.11E+06	259056	1046250	0.9833
peak 59	261815	537898	8.68E+05	1.44E+06	64776	168557	0.9865
				AVERAGE:	431227	AVERAGE	0.9141
				std dev	145940.871		
				%	33.8431547		

Ozone Precursor: Full Concentration Range

Concentration:		0.1	0.25	0.5	1	2.5	5	10	20	SLOPE	INTERCEPT	R2
peak	1											
peak	2	-	--	150661	258410	2.24E+06	4.05E+06	6.13E+06	8.50E+06	426128	784237	0.9123
peak	3	--	137819	237390	416674	1.87E+06	3.57E+06	5.48E+06	8.00E+06	407473	531634	0.9436
peak	4	--	115499	199347	352550	1.78E+06	3.36E+06	5.02E+06	7.01E+06	358832	535012	0.9244
peak	5	--	108585	185938	326148	2.09E+06	3.90E+06	5.81E+06	8.30E+06	425714	571841	0.9285
peak	6	--	112324	211663	369903	1.89E+06	3.56E+06	5.29E+06	7.71E+06	393173	531082	0.9367
peak	7	--	110777	192434	336449	2.90E+06	5.73E+06	8.36E+06	1.12E+07	584338	843993	0.9023
peak	8	112700	213353	367522	656650	4.75E+06	8.58E+06	1.18E+07	1.58E+07	829960	1202178	0.8916
peak	9	170403	327832	555953	978011	2.69E+06	4.98E+06	7.42E+06	1.04E+07	529132	834375	0.9343
peak	10	--	168081	292523	515964	2.44E+06	4.41E+06	6.42E+06	8.87E+06	450756	776618	0.9152
peak	11	--	150079	256547	451842	3.07E+06	5.61E+06	8.34E+06	1.16E+07	596001	866754	0.9178
peak	12	--	189759	330327	592047	2.98E+06	5.54E+06	7.92E+06	9.44E+06	488566	1117481	0.8487
peak	13	--	183759	328678	587986	2.76E+06	5.18E+06	7.22E+06	1.07E+07	539203	826904	0.9309
peak	14	--	174766	306938	541497	3.03E+06	5.49E+06	8.10E+06	1.12E+07	573619	906192	0.9167
peak	15	--	191121	331876	588681	3.97E+06	7.19E+06	1.03E+07	1.37E+07	705475	1226500	0.8943
peak	16	145907	277156	470266	827723	3.32E+06	6.08E+06	8.57E+06	1.14E+07	593382	971903	0.9035
peak	17	108636	212677	364986	641332	3.45E+06	6.23E+06	8.80E+06	1.18E+07	616385	917240	0.9015
peak	18	116830	223658	381898	672944	2.73E+06	5.07E+06	7.51E+06	1.05E+07	543667	726598	0.9287
peak	19	--	164470	283809	500961	3.59E+06	6.45E+06	9.07E+06	1.16E+07	600496	1161312	0.8733
peak	20	115490	227244	394723	689424	3.89E+06	7.12E+06	9.88E+06	1.29E+07	680023	1063038	0.8891
peak	21	126480	247447	427612	760248	3.27E+06	6.02E+06	8.49E+06	1.12E+07	584679	942976	0.8992
peak	22	108060	209130	363828	643529	2.86E+06	5.20E+06	7.85E+06	9.49E+06	504019	860581	0.8772
peak	23	105343	205673	361829	645145	3.72E+06	6.71E+06	9.33E+06	1.21E+07	637500	1015165	0.8852
peak	24	124890	236722	411643	730383	4.05E+06	7.15E+06	1.00E+07	1.30E+07	683287	1109161	0.8861
peak	25											
peak	26	121707	237432	429687	753256	4.05E+06	7.36E+06	1.02E+07	1.32E+07	695164	1127464	0.8856
peak	27	135636	253715	452101	785301	4.06E+06	7.39E+06	1.01E+07	1.32E+07	692066	1147296	0.8857
peak	28	167222	320433	554743	990320	5.00E+06	8.74E+06	1.16E+07	1.43E+07	748585	1518932	0.8492
peak	29	139857	268616	488907	869937	3.98E+06	6.99E+06	9.14E+06	1.15E+07	597465	1226744	0.8549
peak	30	148402	280824	493468	870809	4.37E+06	8.13E+06	1.10E+07	1.43E+07	750993	1260322	0.8828
peak	31	264153	505713	886273	1.56E+06	7.19E+06	1.22E+07	1.57E+07	1.92E+07	1001264	2257699	0.8383
peak	32	171276	328229	575296	1.02E+06	5.29E+06	9.36E+06	1.23E+07	1.58E+07	825992	1545770	0.8662
peak	33	205169	384887	690560	1.22E+06	5.85E+06	9.31E+06	1.15E+07	1.37E+07	713197	1857906	0.8046
peak	34	153538	302371	537625	947066	5.11E+06	8.91E+06	1.17E+07	1.48E+07	776969	1491882	0.8592
peak	35	199707	378292	667778	1.18E+06	6.10E+06	1.09E+07	1.41E+07	1.81E+07	943773	1807516	0.8612
peak	36	187408	368657	643313	1.13E+06	5.63E+06	9.36E+06	1.16E+07	1.40E+07	729573	1779935	0.8138
peak	37	178108	358549	653090	1.17E+06	5.79E+06	9.47E+06	1.12E+07	1.34E+07	696158	1855173	0.7916
peak	38	176314	345283	613023	1.08E+06	5.95E+06	1.02E+07	1.29E+07	1.61E+07	841151	1778834	0.8390
peak	39	184464	352565	626591	1.12E+06	6.16E+06	1.07E+07	1.37E+07	1.75E+07	915575	1792273	0.8557
peak	40											
peak	41	164005	321198	577753	1.03E+06	6.39E+06	1.05E+07	1.28E+07	1.58E+07	827019	1881076	0.8179
peak	42	175718	362684	659609	1.19E+06	5.78E+06	9.75E+06	1.19E+07	1.60E+07	819450	1692529	0.8595
peak	43	172284	344002	626354	1.13E+06	7.09E+06	1.17E+07	1.47E+07	1.60E+07	854892	2260152	0.7608
peak	44	174304	355329	647728	1.15E+06	5.51E+06	9.58E+06	1.21E+07	1.55E+07	805359	1670185	0.8528
peak	45	134389	296952	562328	1.00E+06	6.36E+06	9.47E+06	1.34E+07	1.65E+07	866785	1701943	0.8531
peak	46	151336	314503	561307	1.01E+06	6.11E+06	1.05E+07	1.34E+07	1.67E+07	878548	1774363	0.8417
peak	47	141392	298612	540282	945819	7.20E+06	1.15E+07	1.40E+07	1.70E+07	893138	2054645	0.8031
peak	48											
peak	49											
peak	50	138235	301844	566786	1.00E+06	297926	595140	924737.6	1492420	53154	403678	0.6719
peak	51	111734	253530	483609	856634	6944630	11285100	13908120	17540900	920634	1894665	0.8264
peak	52		323796	598567	1.05E+06	5289400	9542210	12924180	17515600	886447	1779207	0.8912
peak	53		214575	402541	720536	7274570	11907200	14686800	17408600	891952	2515101	0.7800
									AVERAGE	679808	AVERAGE:	0.8685
									std dev	188606.5		
									%	27.74408		

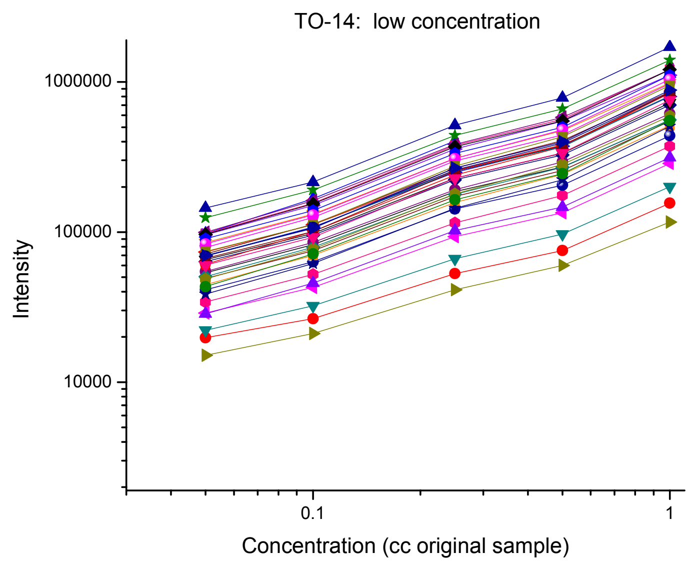
TO-14: low concentration
Intensity
Concentration (cc original sample)
1000000
100000
10000
0.1
1

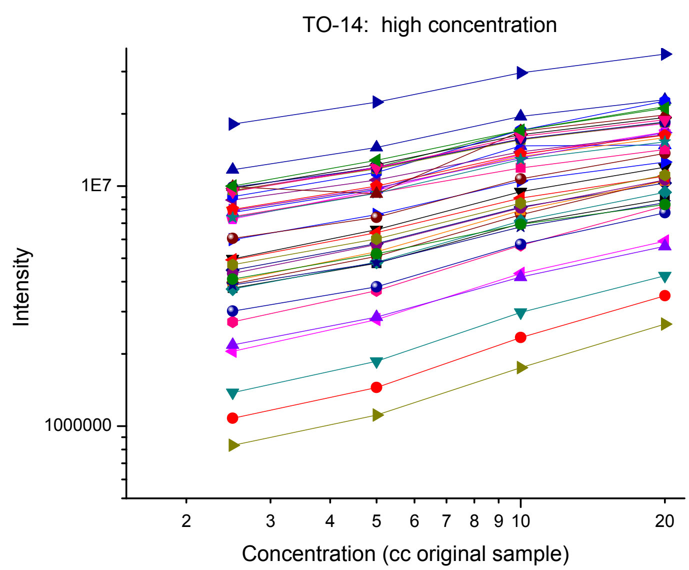
TO-14: high concentration
Intensity
Concentration (cc original sample)
1E7
1000000
2
3
4
5
6
7
8
9
10
20

TO-14: full concentration range

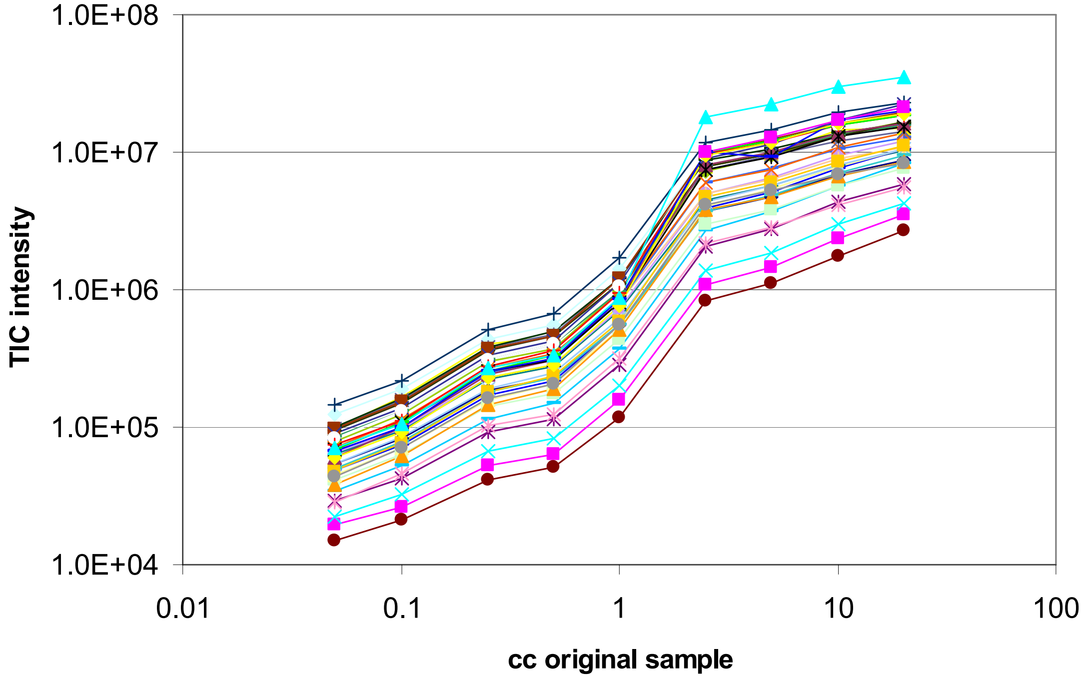

TO-14: Low Concentration

Run #:		Scan	0.05	0.1	0.25	0.5	1	slope	intercept	R2
peak	1	429-30	53452	82363	186086	271522.75	556532	518641	32908	0.9936
peak	2	447-8	19762	26515	52779	75222.75	156052	140915	12518	0.9923
peak	3	468-9	97455	166500	404901		1.13E+06		77582	0.9918
peak	4	477-8	22166	32185	66481	96848.25	200754	184279	13661	0.9935
peak	5	532-3	28861	42776	93088	133993	287081	266114	16037	0.9916
peak	6	566-7	15072	21080	41196	59987.5	116585	104891	10925	0.9955
peak	7	710-1	63661	95484	222635	326331.75	701902	659457	31409	0.9923
peak	8	839-40	49019	75127	172973	256997.75	548668	516278	24371	0.9932
peak	9	890-1	34180	52202	115130	175722.5	372743	350455	16823	0.9945
peak	10	958-9	124349	190647	439727	662241	1.40E+06	1320631	61699	0.9941
peak	11	1127-8	41307	63461	142246	205528.5	438002	408511	22875	0.9920
peak	12	1316-7	44697	69769	156997	242153.75	512588	484524	21122	0.9950
peak	13	1386	54610	85565	191610	293409	615201	580008	27676	0.9951
peak	14	1520-1	28535	45691	102291	147158.25	313545	292784	16186	0.9917
peak	15	1563	65294	97874	228280	334957.5	725473	682189	31144	0.9921
peak	16	1652	73551	111924	256427	380064.5	806360	757222	37921	0.9933
peak	17	1681	69294	107956	250249	372434.5	800372	755051	33142	0.9930
peak	18	1828	50378	79252	178096	270804.75	560239	527159	27433	0.9952
peak	19	1885	78930	125290	297751	444302	971985	922241	33200	0.9924
peak	20	2079-80	48611	77099	179462	282354.5	593135	564953	21450	0.9959
peak	21	2198-9	38604	61722	144098	222987.75	506927	484741	10666	0.9916
peak	22	2215	71423	112878	266228	406124	858895	815033	33397	0.9946
peak	23	2262-3	97720	155898	377720	564081.5	1.21E+06	1149046	44442	0.9932
peak	24	2384-5	43286	71435	164020	245377	553553	525770	15742	0.9908
peak	25	2498-9	144863	215238	516065	783728.5	1.71E+06	1625041	56725	0.9931
peak	26	2648	85080	131534	309769	473998.5	984395	932054	42775	0.9953
peak	27	2752-3	99418	162077	383336	581985	1.21E+06	1145790	51607	0.9949
peak	28	2795-6	95656	150220	356757	549362.5	1.11E+06	1055171	52128	0.9959
peak	29	2800-1	96336	153877	369786	550718	1.21E+06	1148734	39415	0.9922
peak	30	2878-9	60800	101069	239458	370224.5	843350	808974	15570	0.9916
peak	31	2900-1	90139	139061	334798	499492	1.11E+06	1049514	34891	0.9918
peak	32	2907	69655	107224	253782	369814.25	808564	762333	32121	0.9914
peak	33	3263	83342	130258	309037	480100.5	1.04E+06	995053	30993	0.9942
peak	34	3370	74168	112219	274466	431385.75	947613	908307	22814	0.9940
peak	35	3385	69012	107367	258592	391192.25	849301	807721	28159	0.9933
peak	36	3409	66690	100937	253668	376207.25	849259	810014	21547	0.9906
peak	37	3501	60289	92487	228271	337441	757116	720461	21346	0.9908
peak	38									
peak	39	4282-3	69699	106232	266744	399469.25	883663	843093	24786	0.9921
							AVERAGE:	719545	AVERAGE:	0.9931
							std dev	339056.8022		
							%	47.12101516		

TO-14: High Concentration

Concentration		2.5	5	10	20	slope	intercept	R2
peak	1	3.76E+06	4.77E+06	6.96E+06	8.82E+06	285533	3399343	0.95332
peak	2	1.08E+06	1.45E+06	2.34E+06	3.49E+06	137755	798433	0.98961
peak	3	7.77E+06	9.69E+06	1.47E+07	1.48E+07	392657	8055478	0.72953
peak	4	1.38E+06	1.86E+06	2.98E+06	4.23E+06	162332	1089695	0.98011
peak	5	2.05E+06	2.78E+06	4.33E+06	5.89E+06	217611	1722294	0.96968
peak	6	831740	1.11E+06	1.75E+06	2.66E+06	104503	608115	0.99303
peak	7	4.47E+06	5.77E+06	8.18E+06	1.03E+07	326410	4120436	0.95176
peak	8	3.91E+06	5.10E+06	7.59E+06	1.06E+07	379385	3242394	0.98316
peak	9	2.72E+06	3.67E+06	5.67E+06	8.25E+06	313739	2138453	0.98734
peak	10	9.53E+06	1.20E+07	1.71E+07	2.14E+07	670326	8737447	0.95058
peak	11	3.01E+06	3.81E+06	5.73E+06	7.75E+06	270330	2542336	0.97557
peak	12	4.03E+06	5.33E+06	7.92E+06	1.05E+07	365603	3524445	0.9676
peak	13	4.32E+06	5.71E+06	8.12E+06	1.06E+07	349441	3906243	0.96336
peak	14	2.18E+06	2.85E+06	4.18E+06	5.61E+06	193753	1889161	0.97261
peak	15	4.98E+06	6.58E+06	9.46E+06	1.20E+07	391284	4584801	0.95052
peak	16	4.93E+06	6.39E+06	8.90E+06	1.10E+07	335860	4651016	0.94089
peak	17	5.98E+06	7.62E+06	1.05E+07	1.26E+07	365782	5730546	0.92927
peak	18	3.72E+06	4.82E+06	7.15E+06	9.43E+06	322516	3255670	0.96656
peak	19	7.30E+06	9.59E+06	1.35E+07	1.68E+07	525457	6870663	0.94039
peak	20	4.70E+06	6.03E+06	8.49E+06	1.11E+07	360802	4207048	0.9707
peak	21	3.87E+06	4.79E+06	6.76E+06	8.53E+06	263341	3517159	0.95867
peak	22	6.06E+06	7.40E+06	1.07E+07	1.37E+07	437382	5384071	0.96315
peak	23	7.46E+06	9.37E+06	1.19E+07	1.42E+07	368969	7289443	0.93298
peak	24	4.10E+06	5.22E+06	6.94E+06	8.38E+06	235528	3953427	0.93595
peak	25	1.17E+07	1.45E+07	1.95E+07	2.29E+07	623496	11292978	0.92394
peak	26	7.89E+06	9.81E+06	1.33E+07	1.59E+07	446026	7548082	0.93097
peak	27	8.76E+06	1.06E+07	1.39E+07	1.64E+07	421208	8462650	0.93157
peak	28	7.91E+06	9.82E+06	1.31E+07	1.67E+07	493902	7267488	0.96998
peak	29	9.78E+06	1.23E+07	1.64E+07	1.93E+07	524253	9506893	0.92143
peak	30	8.00E+06	1.00E+07	1.36E+07	1.63E+07	460510	7670280	0.92999
peak	31	9.04E+06	1.14E+07	1.71E+07	2.26E+07	769363	7817712	0.96851
peak	32	7.39E+06	9.34E+06	1.29E+07	1.53E+07	440849	7115089	0.91877
peak	33	9.59E+06	1.20E+07	1.57E+07	1.82E+07	474279	9435269	0.91398
peak	34	9.61E+06	1.18E+07	1.56E+07	1.84E+07	486380	9266756	0.92927
peak	35	9.89E+06	1.19E+07	1.57E+07	1.85E+07	480415	9515090	0.93068
peak	36	9.92E+06	9.29E+06	1.69E+07	1.98E+07	625689	8115549	0.86633
peak	37	9.50E+06	1.19E+07	1.61E+07	1.89E+07	520866	9213609	0.91728
peak	38	1.00E+07	1.28E+07	1.71E+07	2.11E+07	614105	9514087	0.94913
peak	39	1.81E+07	2.24E+07	2.96E+07	3.54E+07	953339	17442274	0.93597
					AVERAGE:	413102	AVERAGE:	0.94344
					std dev	172750.92		
					%	0.4181798		

TO-14: Full Concentration Range

concentration		0.05	0.1	0.25	0.5	1	2.5	5	10	20	slope	intercept	R2
peak	1	53452	82363	186086	228251	556532	3.76E+06	4.77E+06	6.96E+06	8.82E+06	468345	773193	0.8613
peak	2	19762	26515	52779	64233	156052	1.08E+06	1.45E+06	2.34E+06	3.49E+06	181439	170022	0.9424
peak	3	97455	166500	404901	463035	1.13E+06	7.77E+06	9.69E+06	1.47E+07	1.48E+07	824117	1859248	0.7603
peak	4	22166	32185	66481	82906	200754	1.38E+06	1.86E+06	2.98E+06	4.23E+06	221788	234700	0.9282
peak	5	28861	42776	93088	114176	287081	2.05E+06	2.78E+06	4.33E+06	5.89E+06	311598	370956	0.9102
peak	6	15072	21080	41196	50885	116585	831740	1.11E+06	1.75E+06	2.66E+06	137744	129892	0.9430
peak	7	63661	95484	222635	275973	701902	4.47E+06	5.77E+06	8.18E+06	1.03E+07	547470	945719	0.8536
peak	8	49019	75127	172973	217811	548668	3.91E+06	5.10E+06	7.59E+06	1.06E+07	555784	706916	0.9053
peak	9	34180	52202	115130	148290	372743	2.72E+06	3.67E+06	5.67E+06	8.25E+06	431095	450715	0.9280
peak	10	124349	190647	439727	561657	1.40E+06	9.53E+06	1.20E+07	1.71E+07	2.14E+07	1140378	1985916	0.8486
peak	11	41307	63461	142246	174748	438002	3.01E+06	3.81E+06	5.73E+06	7.75E+06	407836	566419	0.8937
peak	12	44697	69769	156997	203407	512588	4.03E+06	5.33E+06	7.92E+06	1.05E+07	558183	755883	0.8880
peak	13	54610	85565	191610	247394	615201	4.32E+06	5.71E+06	8.12E+06	1.06E+07	560761	869933	0.8703
peak	14	28535	45691	102291	124873	313545	2.18E+06	2.85E+06	4.18E+06	5.61E+06	296040	419260	0.8887
peak	15	65294	97874	228280	282362	725473	4.98E+06	6.58E+06	9.46E+06	1.20E+07	638978	1026211	0.8623
peak	16	73551	111924	256427	319663	806360	4.93E+06	6.39E+06	8.90E+06	1.10E+07	584405	1082357	0.8399
peak	17	69294	107956	250249	314310	800372	5.98E+06	7.62E+06	1.05E+07	1.26E+07	675116	1286848	0.8193
peak	18	50378	79252	178096	228791	560239	3.72E+06	4.82E+06	7.15E+06	9.43E+06	498197	731651	0.8839
peak	19	78930	125290	297751	375455	971985	7.30E+06	9.59E+06	1.35E+07	1.68E+07	898045	1517078	0.8456
peak	20	48611	77099	179462	237688	593135	4.70E+06	6.03E+06	8.49E+06	1.11E+07	589664	917944	0.8650
peak	21	38604	61722	144098	187688	506927	3.87E+06	4.79E+06	6.76E+06	8.53E+06	454069	776958	0.8451
peak	22	71423	112878	266228	343361	858895	6.06E+06	7.40E+06	1.07E+07	1.37E+07	727744	1213087	0.8579
peak	23	97720	155898	377720	472729	1.21E+06	7.46E+06	9.37E+06	1.19E+07	1.42E+07	756980	1720352	0.7872
peak	24	43286	71435	164020	207205	553553	4.10E+06	5.22E+06	6.94E+06	8.38E+06	448886	888820	0.8099
peak	25	144863	215238	516065	666134	1.71E+06	1.17E+07	1.45E+07	1.95E+07	2.29E+07	1229045	2598026	0.7984
peak	26	85080	131534	309769	403619	984395	7.89E+06	9.81E+06	1.33E+07	1.59E+07	853970	1687362	0.8079
peak	27	99418	162077	383336	492479	1.21E+06	8.76E+06	1.06E+07	1.39E+07	1.64E+07	875004	1946252	0.7834
peak	28	95656	150220	356757	463883	1.11E+06	7.91E+06	9.82E+06	1.31E+07	1.67E+07	884453	1658202	0.8339
peak	29	96336	153877	369786	461963	1.21E+06	9.78E+06	1.23E+07	1.64E+07	1.93E+07	1038628	2117335	0.7965
peak	30	60800	101069	239458	309397	843350	8.00E+06	1.00E+07	1.36E+07	1.63E+07	879317	1651027	0.8085
peak	31	90139	139061	334798	420849	1.11E+06	9.04E+06	1.14E+07	1.71E+07	2.26E+07	1196800	1673105	0.8817
peak	32	69655	107224	253782	311053	808564	7.39E+06	9.34E+06	1.29E+07	1.53E+07	828420	1544749	0.8123
peak	33	83342	130258	309037	403919	1.04E+06	9.59E+06	1.20E+07	1.57E+07	1.82E+07	987024	2067463	0.7812
peak	34	74168	112219	274466	361760	947613	9.61E+06	1.18E+07	1.56E+07	1.84E+07	992074	1998753	0.7883
peak	35	69012	107367	258592	332721	849301	9.89E+06	1.19E+07	1.57E+07	1.85E+07	1001315	2026790	0.7819
peak	36	66690	100937	253668	318752	849259	9.92E+06	9.29E+06	1.69E+07	1.98E+07	1072032	1697419	0.8336
peak	37	60289	92487	228271	285160	757116	9.50E+06	1.19E+07	1.61E+07	1.89E+07	1027822	1923782	0.7968
peak	38						1.00E+07	1.28E+07	1.71E+07	2.11E+07	614105	9514087	0.9491
peak	39	69699	106232	266744	336423	883663	1.81E+07	2.24E+07	2.96E+07	3.54E+07	1923016	3490581	0.7914
										AVERAGE:	726094	AVERAGE:	0.8483
										std dev	349009.8		
										%	0.480667		

Appendix D. Plots and Data of Repeatability Testing

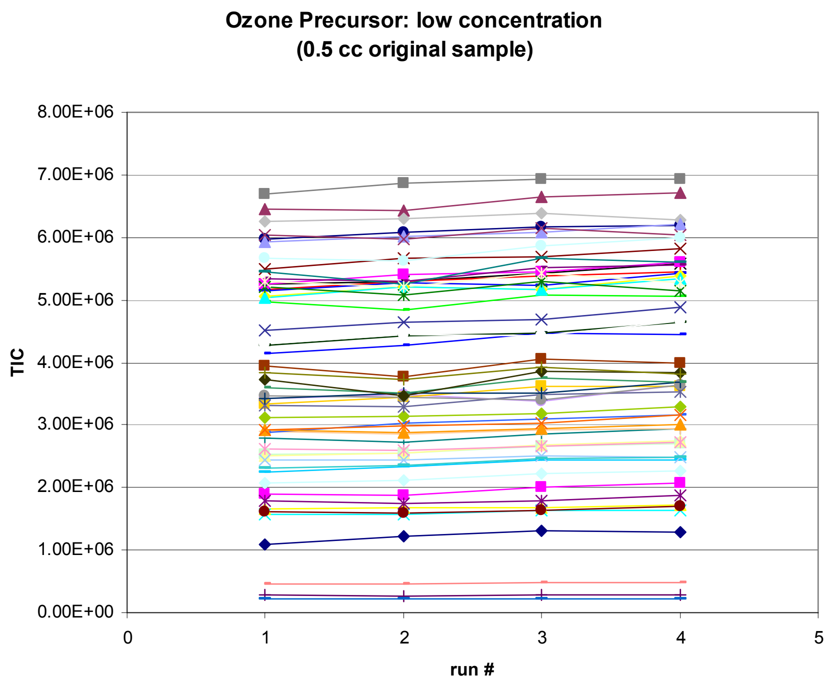

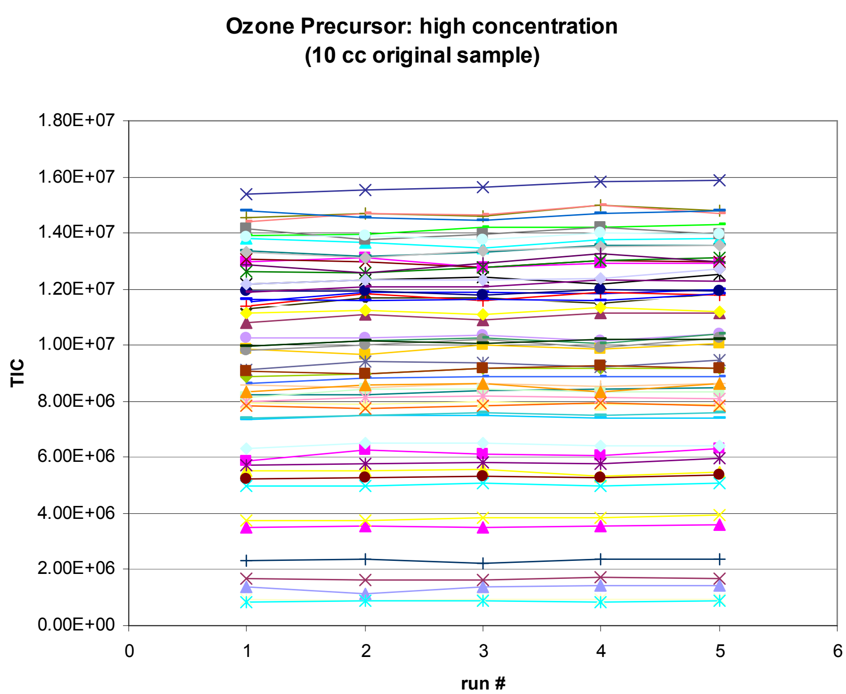

Ozone Precursor: Low Concentration (.5 cc original sample)

Run #:		1	2	3	4	AVERAGE	STDEV	%Dev
peak	1	1.09E+06	1.22E+06	1.32E+06	1.28E+06	1.23E+06	101969	8.32%
peak	2	1.90E+06	1.88E+06	2.01E+06	2.07E+06	1.97E+06	93965	4.78%
peak	3	1.65E+06	1.67E+06	1.67E+06	1.72E+06	1.68E+06	28407	1.69%
peak	4	1.57E+06	1.58E+06	1.64E+06	1.63E+06	1.60E+06	38769	2.42%
peak	5	1.78E+06	1.75E+06	1.79E+06	1.87E+06	1.80E+06	52348	2.91%
peak	6	1.61E+06	1.60E+06	1.64E+06	1.70E+06	1.63E+06	43952	2.69%
peak	7	2.80E+06	2.72E+06	2.85E+06	2.93E+06	2.82E+06	91729	3.25%
peak	8	4.15E+06	4.27E+06	4.46E+06	4.45E+06	4.33E+06	148243	3.42%
peak	9	2.25E+06	2.32E+06	2.43E+06	2.45E+06	2.36E+06	92502	3.91%
peak	10	2.08E+06	2.11E+06	2.23E+06	2.27E+06	2.17E+06	90262	4.16%
peak	11	2.53E+06	2.55E+06	2.65E+06	2.70E+06	2.61E+06	79355	3.04%
peak	12	2.51E+06	2.55E+06	2.68E+06	2.74E+06	2.62E+06	108982	4.16%
peak	13	2.44E+06	2.43E+06	2.50E+06	2.48E+06	2.46E+06	30190	1.23%
peak	14	2.62E+06	2.59E+06	2.65E+06	2.71E+06	2.65E+06	51857	1.96%
peak	15	3.41E+06	3.48E+06	3.38E+06	3.64E+06	3.48E+06	115393	3.32%
peak	16	2.90E+06	2.85E+06	2.93E+06	2.95E+06	2.91E+06	44382	1.53%
peak	17	2.87E+06	3.04E+06	3.10E+06	3.15E+06	3.04E+06	123492	4.06%
peak	18	2.31E+06	2.36E+06	2.46E+06	2.49E+06	2.40E+06	83096	3.46%
peak	19	3.11E+06	3.14E+06	3.19E+06	3.30E+06	3.19E+06	80893	2.54%
peak	20	3.34E+06	3.43E+06	3.62E+06	3.61E+06	3.50E+06	136795	3.91%
peak	21	2.91E+06	2.88E+06	2.94E+06	3.00E+06	2.93E+06	51684	1.76%
peak	22	2.92E+06	2.98E+06	3.04E+06	3.16E+06	3.03E+06	102994	3.40%
peak	23	3.31E+06	3.30E+06	3.48E+06	3.53E+06	3.40E+06	117229	3.44%
peak	24	3.47E+06	3.44E+06	3.39E+06	3.64E+06	3.49E+06	109688	3.15%
peak	25	3.43E+06	3.52E+06	3.51E+06	3.68E+06	3.53E+06	104311	2.95%
peak	26	3.60E+06	3.52E+06	3.75E+06	3.68E+06	3.63E+06	98760	2.72%
peak	27	4.28E+06	4.42E+06	4.47E+06	4.64E+06	4.45E+06	151677	3.41%
peak	28	3.73E+06	3.46E+06	3.87E+06	3.84E+06	3.72E+06	183968	4.94%
peak	29	3.94E+06	3.77E+06	4.05E+06	3.99E+06	3.94E+06	119813	3.04%
peak	30	6.45E+06	6.43E+06	6.66E+06	6.72E+06	6.56E+06	149304	2.27%
peak	31	4.52E+06	4.65E+06	4.69E+06	4.89E+06	4.69E+06	150878	3.22%
peak	32	5.25E+06	5.29E+06	5.44E+06	5.59E+06	5.39E+06	153470	2.85%
peak	33	4.28E+06	4.44E+06	4.43E+06	4.67E+06	4.46E+06	157414	3.53%
peak	34	5.16E+06	5.31E+06	5.39E+06	5.45E+06	5.32E+06	125838	2.36%
peak	35	4.97E+06	4.85E+06	5.09E+06	5.06E+06	4.99E+06	108705	2.18%
peak	36	5.14E+06	5.27E+06	5.24E+06	5.44E+06	5.27E+06	123740	2.35%
peak	37	5.06E+06	5.20E+06	5.17E+06	5.39E+06	5.21E+06	133811	2.57%
peak	38	5.26E+06	5.41E+06	5.45E+06	5.61E+06	5.43E+06	143614	2.64%
peak	39	5.04E+06	5.22E+06	5.16E+06	5.34E+06	5.19E+06	121874	2.35%
peak	40	5.49E+06	5.67E+06	5.68E+06	5.82E+06	5.67E+06	138936	2.45%
peak	41	5.21E+06	5.09E+06	5.29E+06	5.13E+06	5.18E+06	88280	1.70%
peak	42	5.98E+06	6.08E+06	6.17E+06	6.19E+06	6.10E+06	96352	1.58%
peak	43	3.84E+06	3.72E+06	3.93E+06	3.81E+06	3.82E+06	85587	2.24%
peak	44	5.34E+06	5.29E+06	5.51E+06	5.56E+06	5.42E+06	131070	2.42%
peak	45	5.45E+06	5.26E+06	5.67E+06	5.60E+06	5.50E+06	182693	3.32%
peak	46	6.25E+06	6.29E+06	6.38E+06	6.28E+06	6.30E+06	57965	0.92%
peak	47	6.70E+06	6.87E+06	6.92E+06	6.92E+06	6.85E+06	105456	1.54%
peak	48	5.93E+06	6.02E+06	6.08E+06	6.20E+06	6.06E+06	115384	1.90%
peak	49	6.03E+06	5.97E+06	6.14E+06	6.03E+06	6.04E+06	70928	1.17%
peak	50	5.30E+06	5.21E+06	5.43E+06	5.28E+06	5.30E+06	90231	1.70%
peak	51	5.67E+06	5.62E+06	5.86E+06	6.00E+06	5.79E+06	176316	3.05%
peak	52	274049	266865	278450	286779	2.77E+05	8333	3.01%
peak	53	455489	448944	486677	476314	4.67E+05	17629	3.78%
peak	54	208906	209793	214382	220508	2.13E+05	5313	2.49%
							AVERAGE	2.87%

Ozone Precursor: High Concentration (10 cc original sample)

Run #:	1	2	3	4	5	AVERAGE	STDDEV	%Dev
peak 1								
peak 2	5.89E+06	6.24E+06	6.11E+06	6.08E+06	6.31E+06	6.13E+06	160463	2.62%
peak 3	5.50E+06	5.51E+06	5.56E+06	5.34E+06	5.46E+06	5.48E+06	81707	1.49%
peak 4	4.97E+06	4.99E+06	5.10E+06	4.96E+06	5.09E+06	5.02E+06	65371	1.30%
peak 5	5.72E+06	5.79E+06	5.81E+06	5.76E+06	5.95E+06	5.81E+06	88135	1.52%
peak 6	5.21E+06	5.26E+06	5.35E+06	5.26E+06	5.38E+06	5.29E+06	69801	1.32%
peak 7	8.25E+06	8.23E+06	8.38E+06	8.44E+06	8.47E+06	8.36E+06	107956	1.29%
peak 8	1.16E+07	1.19E+07	1.19E+07	1.18E+07	1.20E+07	1.18E+07	162015	1.37%
peak 9	7.33E+06	7.50E+06	7.48E+06	7.39E+06	7.40E+06	7.42E+06	69261	0.93%
peak 10	6.29E+06	6.52E+06	6.50E+06	6.40E+06	6.41E+06	6.42E+06	90562	1.41%
peak 11	8.16E+06	8.43E+06	8.43E+06	8.34E+06	8.32E+06	8.34E+06	111460	1.34%
peak 12	7.94E+06	7.89E+06	8.00E+06	7.88E+06	7.89E+06	7.92E+06	52929	0.67%
peak 13								
peak 14	7.99E+06	8.16E+06	8.16E+06	8.12E+06	8.10E+06	8.10E+06	71099	0.88%
peak 15	1.03E+07	1.03E+07	1.04E+07	1.02E+07	1.04E+07	1.03E+07	88736	0.86%
peak 16	8.56E+06	8.50E+06	8.61E+06	8.56E+06	8.62E+06	8.57E+06	49755	0.58%
peak 17	8.61E+06	8.81E+06	8.87E+06	8.87E+06	8.86E+06	8.80E+06	113798	1.29%
peak 18	7.40E+06	7.50E+06	7.61E+06	7.47E+06	7.60E+06	7.51E+06	86198	1.15%
peak 19	8.87E+06	8.96E+06	9.18E+06	9.15E+06	9.20E+06	9.07E+06	147268	1.62%
peak 20	9.87E+06	9.66E+06	1.00E+07	9.84E+06	1.00E+07	9.88E+06	153330	1.55%
peak 21	8.32E+06	8.56E+06	8.62E+06	8.32E+06	8.62E+06	8.49E+06	156207	1.84%
peak 22	7.84E+06	7.74E+06	7.86E+06	7.96E+06	7.83E+06	7.85E+06	76215	0.97%
peak 23	9.12E+06	9.43E+06	9.39E+06	9.25E+06	9.48E+06	9.33E+06	149076	1.60%
peak 24	9.81E+06	1.00E+07	1.02E+07	9.92E+06	1.03E+07	1.00E+07	191285	1.90%
peak 25	2.34E+06	2.37E+06	2.23E+06	2.35E+06	2.36E+06	2.33E+06	56353	2.42%
peak 26	9.98E+06	1.02E+07	1.03E+07	1.01E+07	1.04E+07	1.02E+07	170757	1.68%
peak 27	9.96E+06	1.02E+07	1.00E+07	1.02E+07	1.02E+07	1.01E+07	109510	1.08%
peak 28	1.13E+07	1.17E+07	1.17E+07	1.15E+07	1.18E+07	1.16E+07	207337	1.79%
peak 29	9.08E+06	8.99E+06	9.16E+06	9.28E+06	9.17E+06	9.14E+06	106046	1.16%
peak 30	1.08E+07	1.11E+07	1.09E+07	1.11E+07	1.11E+07	1.10E+07	155364	1.41%
peak 31	1.54E+07	1.55E+07	1.56E+07	1.58E+07	1.59E+07	1.57E+07	195430	1.25%
peak 32	1.22E+07	1.23E+07	1.24E+07	1.22E+07	1.25E+07	1.23E+07	151094	1.23%
peak 33	1.15E+07	1.13E+07	1.16E+07	1.16E+07	1.17E+07	1.15E+07	158936	1.38%
peak 34	1.14E+07	1.18E+07	1.16E+07	1.19E+07	1.18E+07	1.17E+07	194251	1.66%
peak 35	1.39E+07	1.40E+07	1.42E+07	1.42E+07	1.43E+07	1.41E+07	165540	1.17%
peak 36	1.16E+07	1.16E+07	1.16E+07	1.16E+07	1.18E+07	1.16E+07	108841	0.93%
peak 37	1.11E+07	1.12E+07	1.11E+07	1.13E+07	1.12E+07	1.12E+07	100803	0.90%
peak 38	1.30E+07	1.31E+07	1.28E+07	1.29E+07	1.29E+07	1.29E+07	133304	1.03%
peak 39	1.38E+07	1.36E+07	1.34E+07	1.38E+07	1.38E+07	1.37E+07	151391	1.11%
peak 40	1.31E+07	1.30E+07	1.28E+07	1.30E+07	1.30E+07	1.30E+07	108544	0.84%
peak 41	1.26E+07	1.26E+07	1.28E+07	1.30E+07	1.31E+07	1.28E+07	248301	1.94%
peak 42	1.19E+07	1.19E+07	1.18E+07	1.20E+07	1.20E+07	1.19E+07	85650	0.72%
peak 43	1.45E+07	1.47E+07	1.46E+07	1.50E+07	1.48E+07	1.47E+07	178930	1.22%
peak 44	1.19E+07	1.21E+07	1.21E+07	1.23E+07	1.23E+07	1.21E+07	192267	1.58%
peak 45	1.34E+07	1.32E+07	1.33E+07	1.36E+07	1.36E+07	1.34E+07	171361	1.28%
peak 46	1.33E+07	1.31E+07	1.34E+07	1.35E+07	1.35E+07	1.34E+07	168040	1.26%
peak 47	1.41E+07	1.38E+07	1.40E+07	1.42E+07	1.40E+07	1.40E+07	171532	1.22%
peak 48	1.36E+06	1.15E+06	1.40E+06	1.43E+06	1.43E+06	1.35E+06	118062	8.72%
peak 49	1.69E+06	1.63E+06	1.63E+06	1.73E+06	1.70E+06	1.68E+06	41320	2.46%
peak 50	918185	903745	913655	937521	950582	9.25E+05	18959	2.05%
peak 51	1.39E+07	1.39E+07	1.38E+07	1.40E+07	1.40E+07	1.39E+07	95778	0.69%
peak 52	1.29E+07	1.26E+07	1.29E+07	1.33E+07	1.30E+07	1.29E+07	239559	1.85%
peak 53	1.44E+07	1.47E+07	1.47E+07	1.50E+07	1.47E+07	1.47E+07	217057	1.48%
peak 54	1.48E+07	1.45E+07	1.44E+07	1.47E+07	1.48E+07	1.46E+07	163852	1.12%
peak 55	1.22E+07	1.23E+07	1.23E+07	1.24E+07	1.27E+07	1.24E+07	206845	1.67%
peak 56								
peak 57	3.50E+06	3.55E+06	3.48E+06	3.53E+06	3.59E+06	3.53E+06	40287	1.14%
peak 58	3.76E+06	3.77E+06	3.85E+06	3.86E+06	3.92E+06	3.83E+06	68925	1.80%
peak 59	859326	881808	872502	845785	882139	8.68E+05	15645	1.80%
							AVERAGE	1.51%

Ozone Precursor: low concentration (0.5 cc original sample)

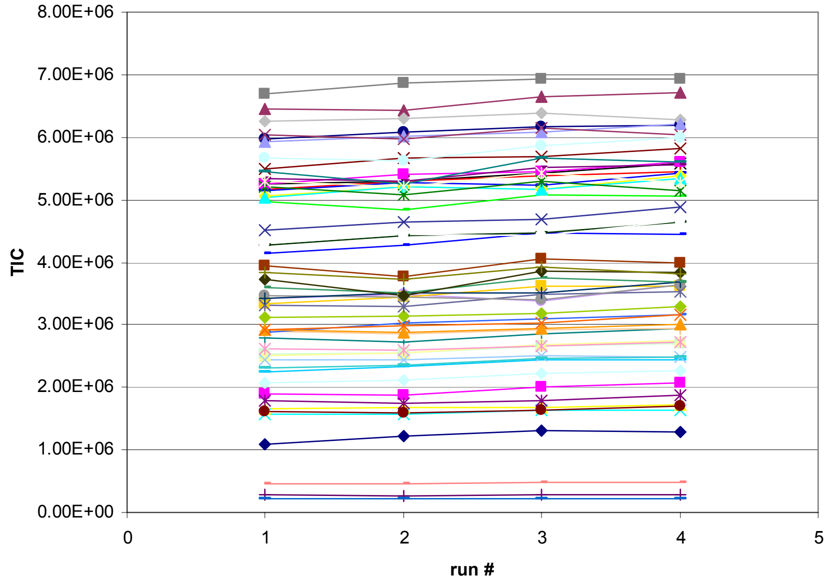

TO-14: high concentration (10 cc original sample)

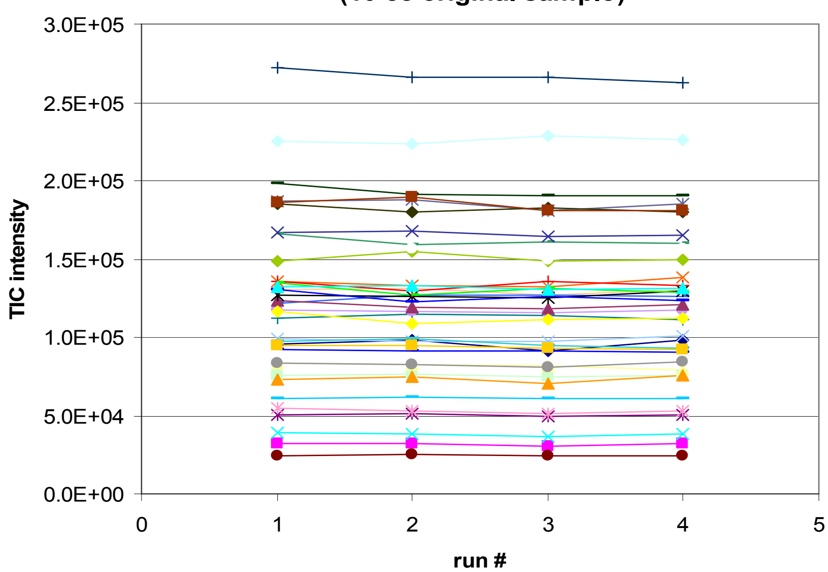

TO-14: Low Concentration (.5 cc original sample)

Run #:	1	2	3	4	AVERAGE	STDEV	%Dev
peak 1	305702	257357	254668	268364	271522.75	23543.9299	8.67%
peak 2	84851	69915	70287	75838	75222.75	6966.95937	9.26%
peak 3							
peak 4	113965	89122	89145	95161	96848.25	11759.6052	12.14%
peak 5	157746	123609	124721	129896	133993	16070.5513	11.99%
peak 6	67967	55576	55782	60625	59987.5	5808.79761	9.68%
peak 7	381109	303736	306756	313726	326331.75	36756.9946	11.26%
peak 8	295861	240469	242958	248703	256997.75	26137.261	10.17%
peak 9	206515	164546	160987	170842	175722.5	20928.8194	11.91%
peak 10	796143	618871	606410	627540	662241	89688.2796	13.54%
peak 11	239805	187549	195848	198912	205528.5	23349.7396	11.36%
peak 12	279913	228848	221643	238211	242153.75	26070.6737	10.77%
peak 13	342030	278388	270147	283071	293409	32851.3164	11.20%
peak 14	169510	137306	138012	143805	147158.25	15182.948	10.32%
peak 15	379532	317856	314467	327975	334957.5	30265.2895	9.04%
peak 16	435681	355935	356322	372320	380064.5	37855.4771	9.96%
peak 17	447584	345989	341633	354532	372434.5	50385.3277	13.53%
peak 18	323003	249371	245403	265442	270804.75	35861.1718	13.24%
peak 19	515615	417956	419864	423773	444302	47603.6111	10.71%
peak 20	326530	267228	262126	273534	282354.5	29817.6639	10.56%
peak 21	265357	208117	204604	213873	222987.75	28503.412	12.78%
peak 22	476377	380551	380479	387089	406124	46937.7587	11.56%
peak 23	641356	532081	530619	552270	564081.5	52455.158	9.30%
peak 24	288330	228052	229076	236050	245377	28854.9901	11.76%
peak 25	930918	734609	726503	742884	783728.5	98353.9615	12.55%
peak 26	560304	443949	444388	447353	473998.5	57556.8593	12.14%
peak 27	691118	532745	547678	556399	581985	73407.999	12.61%
peak 28	646233	506971	517277	526969	549362.5	65094.4985	11.85%
peak 29	644393	508538	509206	540735	550718	64231.5199	11.66%
peak 30	428018	339036	347124	366720	370224.5	40243.9469	10.87%
peak 31	579096	474735	462644	481493	499492	53639.056	10.74%
peak 32	432009	341190	344331	361727	369814.25	42435.5757	11.47%
peak 33	549290	457063	450861	463188	480100.5	46400.0515	9.66%
peak 34	500296	404335	406515	414397	431385.75	46143.0293	10.70%
peak 35	464083	363881	367730	369075	391192.25	48643.6558	12.43%
peak 36	445551	343785	355500	359993	376207.25	46731.3245	12.42%
peak 37	397278	308209	318583	325694	337441	40532.2611	12.01%
peak 38	168371	141008	122604	148475	145114.5	18936.2413	13.05%
peak 39	468351	374572	370316	384638	399469.25	46312.1528	11.59%
						AVERAGE	11.33%

TO-14: High Concentration (10 cc original sample)

Run #:		1	2	3	4	AVERAGE	STDEV	%Dev
peak	1	95277	98393	90969	98552	95797.75	3554.77251	3.71%
peak	2	31879	32249	30118	32119	31591.25	994.052438	3.15%
peak	3							
peak	4	39392	38527	36941	38186	38261.5	1016.1924	2.66%
peak	5	50627	51269	49633	50334	50465.75	678.734791	1.34%
peak	6	24213	25188	24022	24202	24406.25	528.470986	2.17%
peak	7	112289	114510	113782	111508	113022.25	1368.84729	1.21%
peak	8	91955	91588	91150	90491	91296	629.519923	0.69%
peak	9	61111	61585	60829	60626	61037.75	415.516847	0.68%
peak	10	225205	223424	228299	226180	225777	2031.96834	0.90%
peak	11	75789	76289	74704	75532	75578.5	662.327462	0.88%
peak	12	83223	83039	81496	79357	81778.75	1790.61523	2.19%
peak	13	99010	97357	96994	100995	98589	1828.28936	1.85%
peak	14	54663	53241	50951	52911	52941.5	1529.30082	2.89%
peak	15	117591	116849	115719	117093	116813	792.00505	0.68%
peak	16	130712	131422	126995	130746	129968.75	2009.28368	1.55%
peak	17	122035	127300	126567	126438	125585	2396.91872	1.91%
peak	18	97388	98825	95211	92895	96079.75	2591.34938	2.70%
peak	19	148383	154757	148589	149978	150426.75	2972.46703	1.98%
peak	20	94868	94814	93418	92484	93896	1156.10495	1.23%
peak	21	72674	74471	70351	75675	73292.75	2316.61626	3.16%
peak	22	136036	132935	132440	138575	134996.5	2867.73412	2.12%
peak	23	186861	187682	180451	184897	184972.75	3233.03185	1.75%
peak	24	83362	82621	81043	83990	82754	1270.50777	1.54%
peak	25	272504	265977	266029	262662	266793	4120.28454	1.54%
peak	26	165835	158900	160649	160091	161368.75	3065.55056	1.90%
peak	27	198374	191473	190378	190222	192611.75	3881.61568	2.02%
peak	28	185049	179977	182316	180371	181928.25	2318.17707	1.27%
peak	29	185715	189347	180521	180779	184090.5	4241.74316	2.30%
peak	30	123410	118988	118261	120741	120350	2290.22896	1.90%
peak	31	166921	168243	164339	165563	166266.5	1687.70959	1.02%
peak	32	126680	126232	124946	129382	126810	1865.53513	1.47%
peak	33	158462	156244	149565	156913	155296	3931.97618	2.53%
peak	34	135892	129423	136085	133351	133687.75	3104.13803	2.32%
peak	35	135191	126910	131223	129048	130593	3535.06332	2.71%
peak	36	130170	122787	125747	123146	125462.5	3404.21156	2.71%
peak	37	116569	108593	111442	112552	112289	3304.81437	2.94%
peak	38							
peak	39	132452	133176	130258	130980	131716.5	1334.26072	1.01%
							AVERAGE	1.91%

Distribution

Chris Harvey
LLNL, L-091
P.O.Box 808
Livermore, CA 94551

Lorelei Woods
BWXT Pantex, LLC
MS 12-21B
P.O. Box 30020
Amarillo, TX 79120-0020

10	MS 0889	S. Thornberg, 1825
1	MS0889	J. Brown, 1825
1	MS 0889	J. Braithwaite, 1825
1	MS0634	S. Hingorani, 2901
1	MS0634	C. Koenig,2951
2	MS0899	Technical Library, 4536
2	MS9018	Central Technical Files, 8944